Dehydrogenation of n-Alkanes by Solid-Phase Molecular Pincer-Iridium Catalysts. High Yields of α-Olefin Product

ARTICLE *in* JOURNAL OF THE AMERICAN CHEMICAL SOCIETY · JULY 2015

Impact Factor: 12.11 · DOI: 10.1021/jacs.5b05313

7 AUTHORS, INCLUDING:

Akshai Kumar
Indian Institute of Technology Guwahati
15 PUBLICATIONS **23** CITATIONS
SEE PROFILE

Karsten Krogh-Jespersen
Rutgers, The State University of New Jersey
183 PUBLICATIONS **5,403** CITATIONS
SEE PROFILE

Alan S. Goldman
Rutgers, The State University of New Jersey
152 PUBLICATIONS **5,004** CITATIONS
SEE PROFILE

JACS
JOURNAL OF THE AMERICAN CHEMICAL SOCIETY
Article
pubs.acs.org/JACS

Dehydrogenation of *n*-Alkanes by Solid-Phase Molecular Pincer-Iridium Catalysts. High Yields of α-Olefin Product

Akshai Kumar,[†,§] Tian Zhou,[†] Thomas J. Emge,[†] Oleg Mironov,[‡] Robert J. Saxton,[‡] Karsten Krogh-Jespersen,*[,†] and Alan S. Goldman*[,†]

[†]Department of Chemistry and Chemical Biology, Rutgers, The State University of New Jersey, New Brunswick, New Jersey 08903, United States

[‡]Chevron Energy Technology Company, 100 Chevron Way, Richmond, California 94802, United States

[§]Department of Chemistry, Indian Institute of Technology Guwahati, Guwahati - 781039, Assam, India

Supporting Information

ABSTRACT: We report the transfer-dehydrogenation of gas-phase alkanes catalyzed by solid-phase, molecular, pincer-ligated iridium catalysts, using ethylene or propene as hydrogen acceptor. Iridium complexes of sterically unhindered pincer ligands such as $^{i\mathrm{Pr4}}$PCP, in the solid phase, are found to give extremely high rates and turnover numbers for *n*-alkane dehydrogenation, and yields of terminal dehydrogenation product (α-olefin) that are much higher than those previously reported for solution-phase experiments. These results are explained by mechanistic studies and DFT calculations which jointly lead to the conclusion that olefin isomerization, which limits yields of α-olefin from pincer−Ir catalyzed alkane dehydrogenation, proceeds via two mechanistically distinct pathways in the case of ($^{i\mathrm{Pr4}}$PCP)Ir. The more conventional pathway involves 2,1-insertion of the α-olefin into an Ir−H bond of ($^{i\mathrm{Pr4}}$PCP)IrH$_2$, followed by 3,2-β-H elimination. The use of ethylene as hydrogen acceptor, or high pressures of propene, precludes this pathway by rapid hydrogenation of these small olefins by the dihydride. The second isomerization pathway proceeds via α-olefin C−H addition to (pincer)Ir to give an allyl intermediate as was previously reported for ($^{t\mathrm{Bu4}}$PCP)Ir. The improved understanding of the factors controlling rates and selectivity has led to solution-phase systems that afford improved yields of α-olefin, and provides a framework required for the future development of more active and selective catalytic systems.

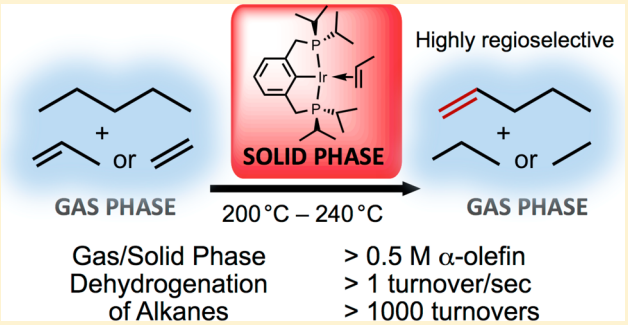

INTRODUCTION

Olefins are key intermediates in many, perhaps even most, processes in the fuel and commodity chemical industries, and are also of great importance in the synthesis of fine chemicals. The development of catalysts for the regioselective dehydrogenation of alkanes and alkyl groups to afford olefins is therefore a goal of great interest to a broad range of chemists.

The most significant progress toward the goal of practical regioselective alkane dehydrogenation catalysts has been realized with pincer-ligated iridium complexes, beginning with the report by Kaska and Jensen[1] of alkane dehydrogenation by ($^{t\mathrm{Bu4}}$PCP)-IrH$_n$ (**1**-**H**$_n$; ^{R4}PCP = κ^3-C$_6$H$_3$-2,6-(CH$_2$PR$_2$)$_2$; n = 2 or 4). Our group subsequently reported the synthesis and generally greater catalytic activity of the less crowded $^{i\mathrm{Pr4}}$PCP analogue (**2**)[2] and soon discovered that both complexes showed kinetic selectivity for dehydrogenation of *n*-alkanes at the terminal position to give the highly desirable corresponding α-olefins.[3] Catalysts **1** and **2** were also found to be effective for the acceptorless dehydrogenation of alkanes.[2,4] Work with these complexes has been followed by reports of numerous catalytically active variants with the (PCP)Ir motif,[5−9] including other bis-phosphines,[10−14] bis-phosphinites (POCOP),[15−18] hybrid phosphine−phosphinites (PCOP),[19,20] arsines (AsOCOAs),[21] hybrid phosphine-thiophosphinites (PSCOP)[22] and hybrid amine-phosphinites (NCOP).[23] In addition to simple alkane dehydrogenation, these complexes have been employed for numerous other catalytic transformations of hydrocarbons, including alkane metathesis,[6,8,9,20,24−26] alkyl group metathesis,[27] dehydroaromatization,[19,28,29] alkane−alkene coupling reactions,[30−32] borylation of alkanes[23] and the dehydrogenation of several non-alkane substrates.[22,33,34] Several pincer motifs more recently explored, such as (CCC)Ir,[35−38] (PCP)Ru,[39−41] (PCP)Os,[42] and (NCN)Ir,[43,44] have been found to show promise for alkane dehydrogenation, but as of yet none have proven to be competitive with the well investigated PCP-type iridium-based systems.[26]

In early alkane dehydrogenation studies,[45] 3,3-dimethyl-1-butene (TBE) was found by Crabtree to be a singularly effective hydrogen acceptor. In addition to being resistant to double-bond isomerization, the bulky TBE is only weakly coordinating; in contrast, ethylene was found to completely inhibit catalytic

Received: May 22, 2015
Published: July 22, 2015

DOI: 10.1021/jacs.5b05313
J. Am. Chem. Soc. 2015, 137, 9894−9911

activity.[45] TBE has thus become the most commonly used acceptor for alkane transfer dehydrogenation.[8,9] We have found that norbornene (NBE) is also very effective, presumably for similar reasons.[3,6] However, on a large scale, the use of smaller olefins, such as ethylene or propene, would be much more practical. Ethylene, in particular, is efficiently dehydrogenated with heterogeneous catalysts which could allow for recycling of ethane (without necessarily requiring the costly separation of ethylene and ethane).[46] We have earlier reported the use of propene as acceptor for dehydroaromatization reactions.[19] Very recently, Brookhart and co-workers have demonstrated the role of ethylene as both an acceptor and a dienophile in the synthesis of piperylene,[47] toluene[47] and *p*-xylene.[48]

The dehydrogenation of lighter alkanes, e.g., butane and pentane,[47,49] is of particular interest. Such alkanes are generally undesirable as transportation fuel components, while the corresponding olefins and dienes have many chemical applications and could potentially be dimerized (or cross-dimerized) to give alkanes of molecular weight more suitable for fuel.[32]

Given these considerations, we were led to study the transfer-dehydrogenation of lighter alkanes using gaseous olefins. At high temperatures, mixtures of these hydrocarbons are entirely in the gas phase, while the catalyst is (at least primarily) in the solid phase.[50] Much to our surprise, the turnover rates resulting from such dual-phase systems were found to be remarkably high. Although heterogeneous solid–gas systems for alkane dehydrogenation are very well known,[46] to our knowledge these are the first examples of purely *molecular* solid-phase catalysts for alkane dehydrogenation. Characteristic of their behavior in solution, and in contrast with nonmolecular solid-phase dehydrogenation catalysts, these systems are selective for the formation of α-olefins. Most remarkably, the maximum yields of α-olefin from these heterogeneous systems are found to be much *greater* than have been previously obtained from homogeneous solution phase systems (the highest previously reported yield being 97 mM 1-octene[3] from the transfer dehydrogenation of *n*-octane with 0.5 M 1-decene catalyzed by **1**-$\mathbf{H}_n$).

RESULTS AND DISCUSSION

A crystalline precursor of ($^{i\mathrm{Pr4}}$PCP)Ir. As initial results (see below) indicated the particular effectiveness of ($^{i\mathrm{Pr4}}$PCP)Ir for our purposes, we explored several synthetic routes to viable precursors of this catalyst (see Experimental and Computational Details section). We successfully obtained crystalline ($^{i\mathrm{Pr4}}$PCP)Ir(C_2H_4) (**2-$\mathbf{C_2H_4}$**), which was characterized by X-ray diffraction (Figure 1). This is the first report of a crystal structure of a direct precursor of the ($^{i\mathrm{Pr4}}$PCP)Ir catalyst.

Transfer Dehydrogenation by Various Pincer–Iridium Complexes: Gas–Solid Phase. In a typical experimental setup (Figure 2), 100 μL of a stock *n*-pentane solution of catalyst (1 mM) was added to a custom-made thick-walled long-neck 1.5 mL ampule inside an argon-filled glovebox. The ampule was then connected to a Kontes adapter via Tygon tubing and degassed on a high-vacuum line. Propene (1.0 atm) was then introduced to the system. The contents of the vials were frozen in liquid nitrogen and the vials were flame-sealed. (The total gas volume before sealing was 3 mL; thus, after condensation, sealing, and warming, the pressure of propene is approximately 2 atm.) The vials were then placed in a preheated aluminum block inside an oven maintained at 240 °C [*note: extreme caution must be exercised during this process, including the use of appropriate safety shields*] and subjected to interval free heating for a stipulated time. The oven

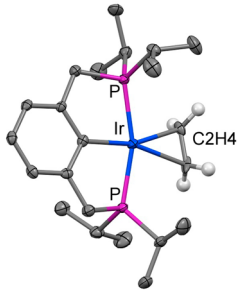

Figure 1. ORTEP diagram of ($^{i\mathrm{Pr4}}$PCP)Ir(C_2H_4) with ellipsoids drawn at the 50% probability level. For the sake of clarity, only H atoms on the ethylene ligand are shown.

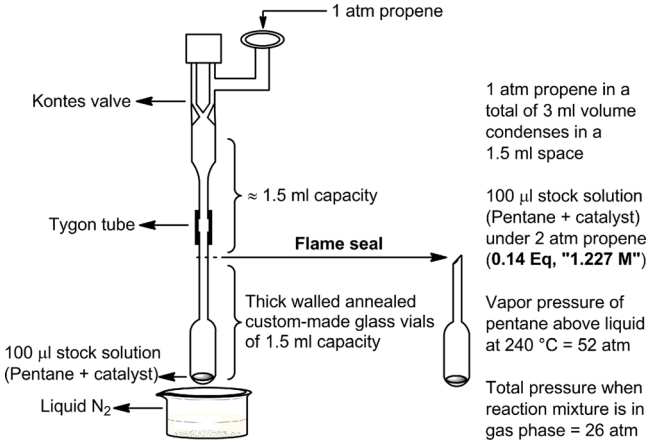

Figure 2. Experimental setup for transfer dehydrogenation of *n*-pentane catalyzed by pincer–iridium complexes using ethylene or propene as acceptor (values given for 2 atm acceptor at 240 °C).

was then cooled to room temperature, the ampules were removed, the contents were frozen in liquid nitrogen, the ampules were broken open, and the contents were analyzed by GC.

The vapor pressure of *n*-pentane at 200 and 240 °C is calculated to be 32 and 52 atm, respectively.[51,52] A volume of 100 μL of *n*-pentane in a 1.5 mL vial, upon converting fully to the gas phase, will generate approximately 22 and 24 atm at 200 and 240 °C, respectively. Thus, all hydrocarbons are expected to be in the gas phase under these conditions.

n-Pentane/propene transfer dehydrogenation was initially investigated with nine different pincer–Ir complexes (Scheme 1 and Table 1). We have previously reported that the relatively uncrowded mixed methyl/*t*-butyl substituted complexes ($^{t\mathrm{Bu3Me}}$PCP)IrH_n (**3**) and ($^{t\mathrm{Bu2Me2}}$PCP)IrH_n (**4**) are catalytically more active than **1** for the transfer dehydrogenation of *n*-octane using either TBE or NBE as acceptor.[6] (Note that under transfer-dehydrogenation conditions, olefin, dihydride and tetrahydride complexes are equivalent as precursors of the catalytically active (pincer)Ir fragments.) Likewise, complexes (*p*-OMe-$^{i\mathrm{Pr4}}$PCP)IrH_4 (**7-$\mathbf{H_4}$**) and ($^{i\mathrm{Pr4}}$PCP)IrH_4 (**2-$\mathbf{H_4}$**) were reported to be more active than **1** for transfer dehydrogenation of *n*-alkanes using TBE.[3,5,49]

Transfer dehydrogenation of gas phase *n*-pentane using propene (2 atm) was successfully catalyzed under these conditions by the relatively crowded complexes ($^{t\mathrm{Bu4}}$PCP)IrH_n (**1**), the *p*-methoxy derivative (*p*-OMe-$^{t\mathrm{Bu4}}$PCP)IrH_n (**5**) and the bisphosphinite complex ($^{t\mathrm{Bu4}}$POCOP)IrH_n (**6**). These catalysts all gave relatively low TO numbers, less than 30 TO after 180 min at 240 °C (entries 1–3, Table 1). The apparent initial

DOI: 10.1021/jacs.5b05313
J. Am. Chem. Soc. 2015, 137, 9894–9911

Scheme 1. Pincer–Ir Catalysts Investigated in This Study

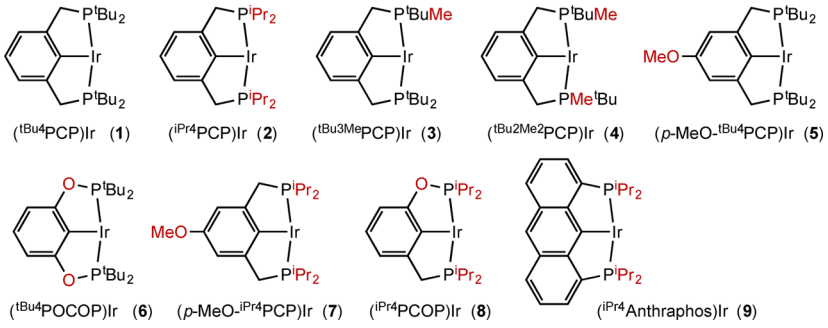

Table 1. Dehydrogenation of *n*-Pentane "[8.7 M]"[a] by Various Pincer–Ir Catalysts, under 2 atm Propene "[1.2 M]"[a] at 240 °C[b]

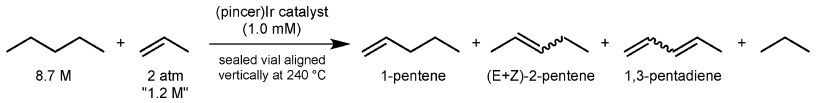

Entry	Catalyst / 1 mM	Time / min	Total Olefins[c] / mM	1-Pentene / mM (% total monoenes)	% Propene conversion (by GC)	Dienes / mM
1	6	10	0	0	ND	0
		180	8	4 (50%)	ND	–
2	1	10	20	15 (75%)	ND	–
		40	20	17 (85%)	ND	–
3	5	10	23	18 (75%)	ND	1
		180	25	20 (77%)	ND	1
4	3	10	0	0	ND	0
		40	59	50 (85%)	ND	0
5	4	10	340	105 (33%)	30	21
		180	950	200 (24%)	98	150
6	2	10	630	140 (24%)	63	40
		180	1050	230 (24%)	90	110
7	8	10	96	53 (56%)	10	2
		180	630	170 (29%)	52	40
8	9	10	110	79 (72%)	ND	2
		180	160	100 (64%)	ND	4
9	7	10	170	120 (70%)	ND	3
		180	310	180 (61%)	ND	10

[a]Concentrations given represent concentrations obtained after the indicated time of heating, followed by cooling of the reaction vessel to 25 °C so that all species are condensed or dissolved into liquid solution phase. [b]Reaction vessels (glass ampules) were oriented vertically. [c]Most runs were repeated; results given are the average of two or more runs. Reproducibility averaged ±3%.

rates with catalysts **1** and **5** were moderately high, but were not maintained over the course of the reaction (e.g., catalyst **1** gave 20 TO after 10 min, but the same TON was found after 40 min). Catalyst **3**, in which one of the ^{t}Bu groups of **1** is substituted by a methyl group, showed slightly greater catalytic activity (entry 4, Table 1; 59 TO after 40 min). To our knowledge, these are the first examples of presumed molecular catalysts effecting heterogeneous (gas–solid phase) dehydrogenation of alkane.

In contrast with the moderate activity noted above, much higher rates and TONs were obtained with the use of catalyst **4**, in which methyl groups replace two of the ^{t}Bu groups of

DOI: 10.1021/jacs.5b05313
J. Am. Chem. Soc. 2015, 137, 9894–9911

Table 2. Dehydrogenation of *n*-Octane [6.2 M][a] by Various Pincer–Ir Catalysts, under 6 atm Propene "[3.7 M]"[a] at 240 °C[b]

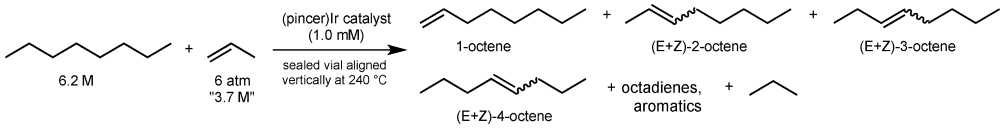

Entry	Catalyst / 1 mM	Time / min	Total Olefins[c] / mM	1-Octene / mM (% total monoenes)	% Propene conversion (by GC)	Dienes / mM
1	 1	10	170	56 (34%)	4	7
		40	190	43 (23%)	4	8
2	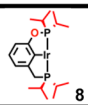 8	10	290	75 (28%)	4	15
		40	600	140 (25)	10	61
3	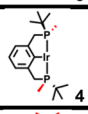 4	10	180	73 (31%)	2	8
		40	1100	140 (16%)	15	260
4	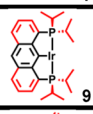 9	10	1250	250 (24%)	15	230
		40	1310	270 (24%)	20	190
5	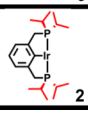 2	10	1930	160 (13%)	44	670
		40	2430	130 (10%)	65	1130

[a]Concentrations given represent concentrations obtained after the indicated time of heating, followed by cooling of the reaction vessel to 25 °C so that all species are condensed or dissolved into liquid solution phase. [b]Reaction vessels (glass ampules) were oriented vertically. [c]Most runs were repeated; results given are the average of two or more runs. Reproducibility averaged ±2%.

1 (entry 5, Table 1). After 10 min, 340 TO had been obtained, corresponding to consumption of ca. 30% of the propene in the vessel, while after 180 min, the TON was 950, corresponding to hydrogenation of >90% of the propene. Dehydrogenation catalyzed by (^{iPr4}PCP)Ir(C_2H_4) (**2**) proceeded even more rapidly (entry 6, Table 1); 630 TO were obtained after 10 min and >1000 TO after 180 min. These rates and turnover numbers are unprecedented even for solution phase alkane dehydrogenation systems.

The very high catalytic efficiency of (^{tBu2Me2}PCP)IrH_4 (**4**) compared to (^{tBu3Me}PCP)IrH_4 (**3**) contrasts with our earlier observations on *n*-octane transfer dehydrogenation with TBE or NBE as acceptors.[6] Studies on **3** and **4** for *n*-octane transfer dehydrogenation using TBE or NBE indicated that **3** was the more effective of the two catalysts (although both **3** and **4** provided higher activity than **1**). However, as **4** showed a tendency to form dinuclear clusters, it was unclear whether this was responsible for its lesser activity. Given the presumably much greater binding ability of propene vs the bulkier TBE or NBE, the formation of dimers or oligomers should be much less significant in the presence of propene; the much greater reactivity of **4** vs **3** when using propene thus lends support to this explanation for the lesser activity of **4** obtained when NBE or TBE is used as acceptor. Another possible explanation, also based on decreased dimerization of **4** under the present conditions, is that catalyst mobility is reduced in the solid phase compared with the solution phase thereby inhibiting the kinetics of dimer formation.

The activity levels of hybrid phosphine-phosphinite catalyst (^{iPr4}PCOP)Ir(C_2H_4) (**8**) (entry 6, Table 1), and (^{iPr4}Anthraphos)Ir(C_2H_4) (**9**) (entry 7, Table 1) were high, but less than those of either **4** or **2**. The *p*-methoxy derivative of **2**, (*p*-OMe^{iPr4}PCP)Ir(C_2H_4) (**7**) appeared to give a good initial rate (170 TO after 10 min) but much lower conversion than **2** after 180 min. We suspect this is due to intermolecular reactions involving the methoxy groups, leading to catalytically inactive species.[53,54]

The great differences in catalytic activity among these various catalysts, and particularly the disparity between the more crowded (three or more *t*-Bu groups) and less crowded complexes, was not expected. Previous studies in our lab and others have indicated that less crowded complexes did indeed tend to be more active, but the difference was much less dramatic. These studies generally utilized NBE and TBE as hydrogen acceptors and, of course, were in the liquid phase. For example, the difference between the activity of ^{tBu4}PCP and ^{iPr4}PCP catalysts was found to be a factor of ca. 3-fold.[6] The present results therefore raised the question as to whether the large differences between the catalysts, most notably the ^{tBu4}PCP and ^{iPr4}PCP derivatives, were a result of the different acceptors used in this study, or a result of the unusual conditions, particularly the solid vs solution phase.

Accordingly, we conducted *solution-phase* experiments (using *n*-octane as dehydrogenation substrate) under similar conditions, including the nature of the acceptor and the unusually high temperature (240 °C). Results are shown in Table 2. A very pronounced difference in activity is observed between the (^{tBu4}PCP)Ir and (^{iPr4}PCP)Ir precursors: a factor of ca. 11 in the initial data point, a value which is of the same magnitude as the factor of ca. 30 observed in the gas–solid-phase experiments. Further, we find that in the case of catalyst **1** and propene as acceptor, in both solid and liquid phases the rate decreases dramatically after an initial period of catalysis with a relatively slow rate. We are not able to fully explain this behavior of catalyst **1**, but our observations all seem applicable to both solution and solid phase. Indeed, the fact that we observe, in both solution and solid phase, both the dramatic difference between catalysts **1** and **2** and the particular temporal profile of catalyst **1**, strongly

DOI: 10.1021/jacs.5b05313
J. Am. Chem. Soc. 2015, 137, 9894–9911

Table 3. Dehydrogenation of *n*-Pentane "8.7 M"[a] under 2 atm Propene "1.2 M"[a] at 240 °C with Selected Catalysts and Ampules Positioned Horizontally[b]

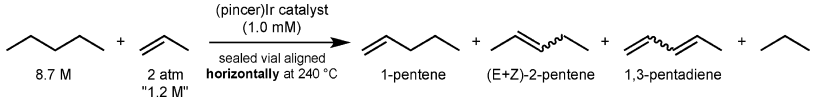

Entry	Catalyst / 1 mM	Time / min	Total Olefins[c] / mM	1-Pentene / mM (% total monoenes)	% Propene conversion (by GC)	Dienes / mM
1	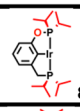 **8**	10	220	120 (54%)	21	3
		180	920	170 (20%)	74	82
2	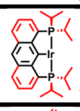 **9**	10	520	240 (50%)	48	32
		180	680	190 (31%)	67	64
3	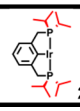 **2**	10	1090	200 (20%)	97	110
		180	1200	190 (17%)	97	114

[a]Concentrations given represent concentrations obtained after the indicated time of heating, followed by cooling of the reaction vessel to 25 °C so that all species are condensed or dissolved into liquid solution phase. [b]Reaction vessels (glass ampules) were oriented horizontally. [c]Most runs were repeated; results given are the average of two or more runs. Reproducibility averaged ±1%.

Table 4. Dehydrogenation of *n*-Butane (3 atm) "[6.1 M]"[a] with Propene (3 atm) "[6.1 M]"[a] at 240 °C Catalyzed by 2[b]

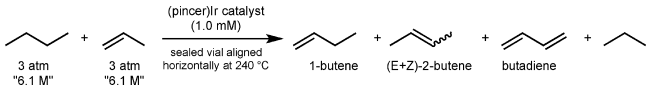

Catalyst / 1 mM	Time / min	Total Olefin[c] / TON	Butadiene / TON	1-Butene / TON	1-Butene Fraction / %
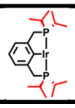	10	335	40	185	65
	40	590	40	370	65
	180	680	65	280	45

[a]Concentrations given represent concentrations obtained after the indicated time of heating, followed by cooling of the reaction vessel to −15 °C so that all species are condensed or dissolved into liquid solution phase. [b]Reaction vessels (glass ampules) were oriented horizontally.

indicates that the catalysts are operating as discrete molecular species even in the solid phase.

In an effort to determine the physical distribution of catalyst during the gas−solid phase experiments, after several runs the GC oven temperature was cooled from 240 to 60 °C and slowly opened in the range of a camcorder (see Supporting Information for images of one such experiment with (^{iPr4}PCP)-Ir(C_2H_4) (**2**)). At this point the top portion of the vial was cool relative to the base, which was still hot as it was enclosed in the aluminum block. The resulting images (Figure S7) clearly show bright red droplets formed along the topmost portions of the vial as pentane condenses on the catalyst that had deposited on the glass. This observation could be explained by vigorous splashing, when the pentane solution is heated to 240 °C (followed by rapid solvent evaporation) or alternatively, by sublimation of the catalyst at this temperature. To distinguish between these possibilities, an ampule containing solid catalyst was heated under the same conditions as the catalytic runs, including the presence of 2 atm propene but in the absence of pentane or other liquid. Under such conditions, no significant migration of the iridium complex within the ampule was observed. Thus, rather than sublimation of catalyst, it seems likely that when a pentane solution of catalyst is heated at 240 °C, the solution splashes and coats the glass surface before the solvent is fully evaporated.

If it is assumed that the catalyst coats the glass surface; then, by having vials aligned horizontally rather than vertically, the catalyst would have a greater surface area and should function more efficiently. When the ampules were positioned horizontally (using catalysts **2**, **8**, and **9** which proved most effective in the experiments, cf. Table 1) even higher rates were achieved as shown in Table 3. Remarkably, in the case of catalyst **2**, the reaction had effectively proceeded to completion (≥97% consumption of propene, >1000 TO) after 10 min.

n-Butane was also investigated as a dehydrogenation substrate. Into an ampule containing the same quantity of catalyst **2** that was used in the experiments of Tables 1−3 was condensed a 1:1 butane/propene gas mixture (see Figure 2) such that upon sealing and warming to room temperature the pressures of butane and propene each reached 3 atm. High rates and turnover numbers were observed (Table 4). In view of the much higher volatility of butane (bp = −1 °C) than pentane (bp = 36 °C), these results may be interpreted as arguing against the possibility of a condensed amorphous catalyst/alkane phase as opposed to a "true" solid−gas interaction. (It is well beyond the scope of this work, however, to address in detail the question of the "phase" of any hydrocarbon adsorbed to the solid.)

Ethylene would be even more attractive as a hydrogen acceptor than propene (in addition to the abundance of ethylene derived from shale gas in North America, ethane could be more easily recycled via separation from the alkane substrate and conventional dehydrogenation methods[46]). In this context, experiments with ethylene gave highly encouraging results (Table 5), although rates were roughly a factor of 10 slower than when propene was used as acceptor.

DOI: 10.1021/jacs.5b05313
J. Am. Chem. Soc. 2015, 137, 9894−9911

Table 5. Dehydrogenation of *n*-Pentane "8.7 M"[a] with Ethylene (2 atm, "1.2 M")[a] at 240 °C[b] by Various Pincer–Ir Catalysts

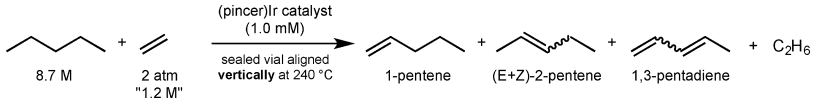

Entry	Catalyst / 1 mM	Time / min	Total Olefins[c] / mM	1-Pentene / mM (% total monoenes)	% Ethylene conversion (by GC)	Dienes / mM
1	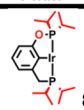 8	10	17	12 (71%)	ND	0
		40	45	34 (76%)	ND	0
2	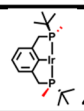 4	10	98	70 (71%)	ND	1
		180	254	135 (55%)	ND	7
3	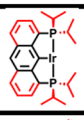 9	10	41	36 (88%)	ND	0
		180	150	120 (78%)	ND	1
4	 7	10	41	36 (88%)	ND	0
		180	156	120 (78%)	ND	1
5	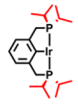 2	10	72	60 (88%)	4	2
		40	320	250 (79%)	ND	5
		100	660	430 (65%)	ND	28
		180	720	420 (61%)	44	41

[a]Concentrations given represent concentrations obtained after the indicated time of heating, followed by cooling of the reaction vessel to 25 °C so that all species are condensed or dissolved into liquid solution phase. [b]Reaction vessels (glass ampules) were oriented vertically. [c]Most runs were repeated; results given are the average of two or more runs. Reproducibility averaged ±2%.

Selectivity for Production of α-Olefins. Regioselective functionalization of the terminal position of *n*-alkanes (or *n*-alkyl groups) has long been one of the major goals of research in catalytic hydrocarbon conversion. Ever since the earliest examples of organometallic C–H bond activation revealed selectivity for oxidative addition at 1° vs 2° positions,[55] and thus a remarkable preference for cleaving stronger C–H bond, this selectivity has been viewed as perhaps the most important potential advantage of "homogeneous" vs "heterogeneous" catalysts for the functionalization of alkanes or alkyl groups. Thus, we were quite surprised to observe that the heterogeneous systems described above appeared to show *greater* selectivity for the formation of α-olefins than the homogeneous (solution-phase) systems based on the same catalysts. For example, **2**-catalyzed pentane–ethylene transfer dehydrogenation yielded 430 mM α-olefin (upon condensation to the liquid phase; entry 5, Table 5) and formation of 660 mM total olefin. This is an unprecedented yield of α-olefin from *n*-alkane dehydrogenation; as noted above, to our knowledge the highest yield of α-olefin previously reported from *any* catalytic alkane dehydrogenation system was 97 mM (out of a total conversion to olefin of 143 mM).[56]

The high selectivity, in even a qualitative sense, for α-olefin formation resulting from a heterogeneous system is certainly noteworthy; for example, after 10 min at 240 °C, 88% selectivity with total conversion to 72 mM (upon condensation) is obtained (entry 5, Table 5). This observed regioselectivity certainly supports the argument that the catalyst, although not in solution, is still operating as a discrete molecular species. But even more remarkable is the appearance of even *greater* selectivity for α-olefin formation from the heterogeneous system as compared with the same catalyst in solution. Accordingly, further experiments were conducted in large part with an aim toward explaining this phenomenon.

When propene pressure is varied from 2 to 4 atm at 240 °C (Table 6), the overall rate of dehydrogenation increases by ca. 2-fold. Further increase in propene pressure to 6 atm results in a decreased rate, which is comparable to the rate observed with 2 atm of propene. The yield of α-olefin, however, depends significantly upon propene pressure; for example, after 40 min at 240 °C, conversion was very similar at 2 and 6 atm propene (850–870 mM), but yields of α-olefin were quite different, 170 mM (22%) and 400 mM (51%), respectively. Reducing the amount of pentane to 50 μL allowed us to have approximately "7.4 M" propene while working under 6 atm (entry 4, Table 6). This reaction system, when heated at 240 °C for 80 min, gave the highest yield of 1-pentene yet reported from transfer-dehydrogenation, ca. 575 mM, which is about 5.9 times greater than the α-olefin yields obtained in previous reports.[3] At lower temperatures, a similar dependence of propene pressure on yields of 1-pentene was observed (entries 5, 6 and 7, Table 6) as illustrated in Figure 3.

Origin of the High α-Olefin Yields. As discussed above, high yields of α-olefin are obtained when using ethylene as acceptor and under high pressures of propene in particular. Both olefins, but ethylene in particular, are expected to bind strongly to the pincer–iridium complex. This strong binding explains the relatively low rate of dehydrogenation obtained in the presence of ethylene, given that (pincer)Ir(ethylene) is presumably not catalytically active. We have recently shown that the dehydrogenation catalyst ($^{t\mathrm{Bu4}}$PCP)Ir (**1**) catalyzes olefin isomerization via an η^3-allyl pathway which, in turn, proceeds via C–H addition prior to olefin coordination.[57] Thus, olefins like ethylene that bind very strongly, or high pressures of propene which binds fairly strongly, would be

DOI: 10.1021/jacs.5b05313
J. Am. Chem. Soc. 2015, 137, 9894–9911

Table 6. Dehydrogenation of *n*-Pentane [8.7 M][a] under 2 and 6 atm Propene at 200 and 240 °C Catalyzed by 2-C_2H_4[b]

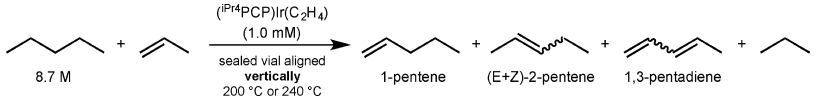

entry	conditions	time/min	total olefins/mM[c]	1-pentene/mM (% total monoenes)	% propene conversion (by GC)	dienes/mM
1	240 °C	10	630	140 (24%)	63	40
	2 atm	40	850	170 (22%)	77	70
	"1.2 M"	180	1050	230 (24%)	90	110
2	240 °C	10	1370	420 (37%)	56	210
	4 atm	40	1450	440 (36%)	66	230
	"2.5 M"	180	1590	430 (33%)	73	290
3	240 °C	10	700	300 (48%)	20	76
	6 atm	40	870	400 (51%)	20	87
	"3.7 M"	180	1060	440 (46%)	30	116
4	240 °C	10	695	380 (58%)	8	40
	6 atm	40	930	485 (56%)	10	65
	"7.4 M"[d]	80	1420	575 (46%)	16	170
5	200 °C	10	410	150 (41%)	36	34
	2 atm	40	690	190 (32%)	60	75
	"1.2 M"	180	720	190 (30%)	67	74
6	200 °C	10	370	155 (46%)	15	30
	4 atm	40	510	210 (45%)	20	40
	"2.5 M"	180	800	260 (37%)	39	94
7	200 °C	10	270	130 (50%)	ND	17
	6 atm	40	470	220 (50%)	14	30
	"3.7 M"	180	950	320 (40%)	35%	110

[a]Concentrations given represent concentrations obtained after the indicated time of heating, followed by cooling of the reaction vessel to 25 °C so that all species are condensed or dissolved into liquid solution phase. [b]Reaction vessels (glass ampules) were oriented vertically. [c]Most runs were repeated; results given are the average of two or more runs. Reproducibility averaged ±3%. [d]Volume of pentane in each vial was reduced from 100 to 50 μL; thus the propene/pentane ratio was doubled.

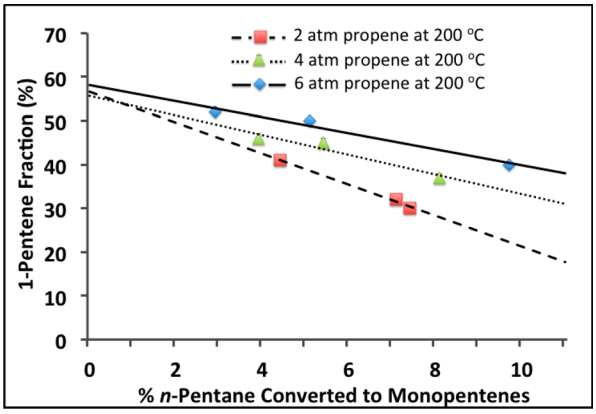

Figure 3. Plot of 1-pentene as fraction of pentenes formed in the dehydrogenation of *n*-pentane catalyzed by **2-C_2H_4** under 2, 4, and 6 atm propene at 200 °C.

expected to inhibit isomerization of the α-olefin primary product. However, such binding of the acceptor olefins would also be expected to inhibit (equally) the rate of dehydrogenation; if the rate of isomerization relative to dehydrogenation were unchanged, the maximum concentration of α-olefin would also be unchanged (although it would of course take more time to reach that maximum).

The conclusion, in our earlier study, of an η^3-allyl isomerization pathway being operative for catalyst **1** was based on several lines of evidence.[57] In particular, we gave very strong consideration to the most commonly proposed pathway for olefin isomerization: insertion into an M–H bond (e.g., 2,1-addition of 1-alkene), followed by β-H migration at C3 to give the more stable double-bond isomer, 2-alkene); we will refer to this as a "hydride addition pathway". Under the conditions of our studies, the only observable resting state was always (^{tBu4}PCP)-Ir(1-alkene). Thus, a hydride addition pathway would proceed via a small, if unobservable, concentration of a catalytically active hydride, most likely (^{tBu4}PCP)IrH_2, which should be present according to eq 1.

$$\text{(pincer)Ir(1-alkene)} + \text{alkane} = \text{(pincer)}IrH_2 + \text{1-alkene} + \text{alkene}' \quad (1)$$

The concentration of the hydride species would be much greater in alkane than in arene solvent due to the steady state of eq 1; therefore, isomerization rates would be commensurately much greater if such a species were largely responsible for isomerization. In fact, we found that rates of 1-alkene isomerization by **1** were identical in *n*-octane and *p*-xylene solvent[57] (and this result was reproduced during the present study).

In the case of (^{iPr4}PCP)Ir (**2**), as with **1**, the major resting state in the presence of any appreciable concentration of 1-alkene is the 1-alkene complex (or the propene or ethylene complex in the presence of these olefins). However, the effect of alkane vs arene solvent on the rate of isomerization proved to be very different in the case of **2**. Addition of 1-octene [100 mM] to **2-C_2H_4** (1 mM) in either *n*-octane or *p*-xylene solvent resulted in complete conversion to (^{iPr4}PCP)Ir(1-octene), *without any hydride species observable in either solvent*. However, in contrast with the catalytic behavior of **1**, 1-octene isomerization is indeed significantly faster in *n*-octane than in *p*-xylene, by ca.

DOI: 10.1021/jacs.5b05313
J. Am. Chem. Soc. 2015, 137, 9894–9911

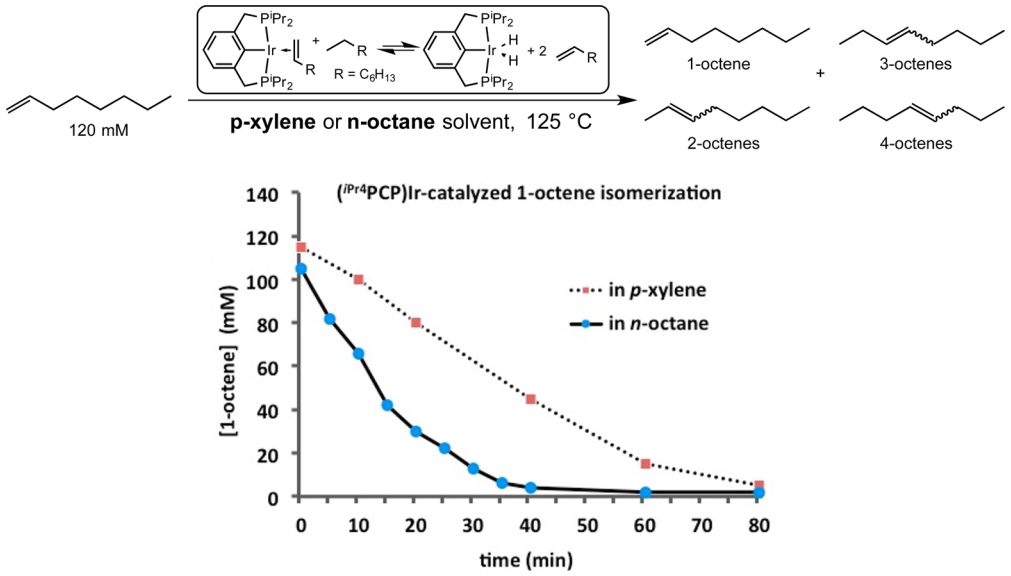

Figure 4. Isomerization of 1-octene in *n*-octane and *p*-xylene at 125 °C catalyzed by **2**.

2-fold (Figure 4). This indicates that dihydride **2-H$_2$** is a much more active catalyst (on a per mole basis) than **2-(1-octene)**. Nevertheless, given that the small concentration of dihydride would be many times greater in alkane than in arene eq 1, the fact that there is *only* a ca. 2-fold difference indicates that isomerization by **2** does not proceed exclusively via the hydride pathway. Instead, it can be concluded that the observed isomerization in *p*-xylene solvent is not due to a hydride pathway, but is presumably due to an allyl pathway; the rate of this pathway might be considered a "baseline", while the presence of any **2-H$_2$** could add to this baseline rate.

Ethylene is presumably a better hydrogen acceptor than propene, given that the thermodynamics of its insertion and hydrogenation are more favorable, and that it is sterically less demanding. Thus, any contribution to isomerization from a hydride pathway would be expected to be minimized by the presence of ethylene, particularly at high pressure. Indeed, under 4 atm ethylene (and with the reaction ampule oriented horizontally so as to maximize surface area and minimize diffusion limitations), the yield of 1-pentene was the highest we have obtained to date, 520 mM (after condensation) after 180 min (entry 2, Table 7). Figure 5a illustrates that at a given conversion level, the fraction of 1-pentenes is significantly higher when ethylene is the acceptor instead of propene. The apparent suppression of isomerization via the hydride pathway is apparently maximized even at only 2 atm ethylene; thus, at a higher ethylene pressure (4 atm), the 1-pentene fraction is not significantly greater, at a given conversion level, than under 2 atm ethylene (Figure 5b).

With 2 atm instead of 4 atm ethylene (entry 1, Table 7), the reaction rate is expected to be somewhat (up to 2-fold) faster due to decreased inhibition. Surprisingly, however, under these conditions the reaction was found to be ca. *4-fold* faster. We suspect this result is due to a diffusion limitation which lowers the local ethylene concentration and thus (somewhat counterintuitively) produces a rate even faster than would be predicted. With respect to mechanistic study, the value of this experiment is thus doubtful.

Overall, the picture that emerges from these studies is illustrated in Scheme 2.

Implicit in the above explanation of selectivity is a model of reactivity that is at least qualitatively not different from the behavior of the catalyst in solution. We therefore further explored the liquid phase reactivity with the same acceptors and *n*-alkanes as an obvious test of this model. Moreover, the solution phase does not present the issue of irreproducible surface area and physical distribution of the catalyst, thus allowing a more rigorously quantitative study of the reaction kinetics.

2-catalyzed, solution-phase, transfer dehydrogenation of *n*-octane was conducted with ethylene and with propene as acceptor. As with the gas−solid phase reactions, a glass ampule was charged with catalyst, alkane, and olefin acceptor, and then sealed. The ampule was rotated in the oven to promote gas−liquid mixing. Transfer-dehydrogenation was run with 2, 4, and 6 atm propene pressure. Higher propene pressures resulted in somewhat lower rates, indicating that a significant fraction of the catalyst was present as the out-of-cycle species **2-propene**. The effect on the rate from a 3-fold increase in $P_{propene}$, however, was less than a factor of 3 (<2-fold), suggesting that **2- propene** is not the only major species present.

If we assume that **2-propene** is catalytically inactive with respect to both octane dehydrogenation and 1-alkene isomerization, then an increase in [**2-propene**] (effectuated by increasing the propene pressure) is expected to lower the rates of both processes equally. Assuming that fragment **2** can react with either *n*-alkane (leading to dehydrogenation) or with α-olefin (leading to isomerization), an increase in $P_{propene}$ would not be expected to have any direct effect on the ratio of dehydrogenation to isomerization if these were the only paths leading to dehydrogenation and isomerization, respectively. In that case, at a given level of conversion (i.e., after dehydrogenation had proceeded to a given extent), the degree of isomerization would be proportional, and the fraction of unisomerized 1-alkene product formed would be independent of propene pressure. However, as seen in Table 8 and Figure 6a, at any given level of conversion the fraction of α-olefin is in fact higher under the higher propene pressure[s]. This is explained in terms of the left side of Scheme 2: if a small concentration of **2-H$_2$** is responsible for a significant fraction of the isomerization, then increasing propene concentration will

DOI: 10.1021/jacs.5b05313
J. Am. Chem. Soc. 2015, 137, 9894−9911

Table 7. Dehydrogenation of *n*-Pentane [8.7 M] with Ethylene at 240 °C Catalyzed by 2.[a,b]

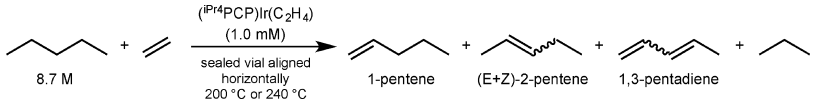

entry	conditions	time/min	total olefins/mM[c]	1-pentene/mM (% total monoenes)	% ethylene conversion (by GC)	dienes/mM
1	240 °C	10	560	350 (64%)	63	24
	2 atm	40	1290	115 (10%)	100	82
	"1.2 M"					
2	240 °C	10	130	114 (88%)	8	0
	4 atm	40	310	240 (79%)	16	4
	"2.4 M"	180	1100	520 (52%)	60	90
3	200 °C	10	26	22 (85%)	85%	0
	2 atm	40	114	90 (80%)	80%	0
	"1.2 M"	80	260	190 (72%)	24	3
		180	420	250 (61%)	61%	14
4	200 °C	10	3	3 (>97%)	ND	0
	4 atm	80	28	26 (93%)	1	0
	"2.4"	600	220	170 (78%)	8	3
		1200	460	280 (64%)	15	11

[a]Concentrations given represent concentrations obtained after the indicated time of heating, followed by cooling of the reaction vessel to 25 °C so that all species are condensed or dissolved into liquid solution phase. [b]Reaction vessels (glass ampules) were oriented horizontally. [c]Most runs were repeated; results given are the average of two or more runs. Reproducibility averaged ±3%.

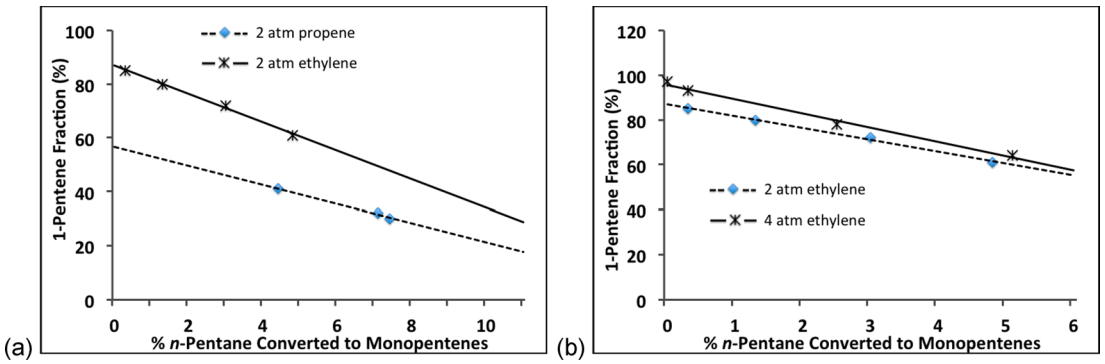

Figure 5. Plot of 1-pentene as percentage fraction of pentenes formed in the dehydrogenation of *n*-pentane catalyzed by **2**-C_2H_4 at 200 °C under (a) 2 atm propene and ethylene, (b) 2 and 4 atm ethylene.

Scheme 2

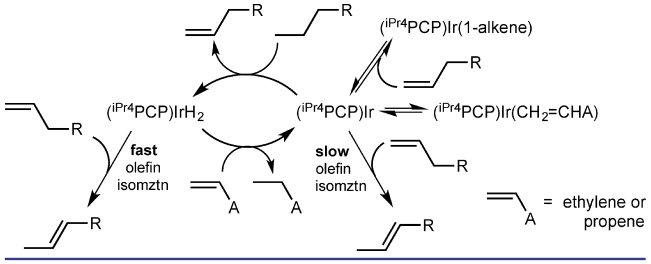

decrease the steady-state concentration of **2**-H_2, thus resulting in decreased isomerization and higher α-olefin yields.

When ethylene is used as the hydrogen acceptor, the yields of 1-octene show a weak dependence on ethylene pressure. At high ethylene pressures, the yields of 1-octene are somewhat higher than those of propene, but the difference between the two acceptors is not large. We interpret these results as approaching a regime where the concentration of **2**-H_2 is too low to contribute significantly to isomerization; in such a regime, the ratio of dehydrogenation to isomerization should be independent of ethylene or propene concentration.

The reaction of *n*-octene with propene is probably too fast at 180 °C to obtain good kinetics data. For this reason, and also to investigate the effect of temperature further, we also conducted runs under propene at 160 °C. We also varied temperature with ethylene as acceptor, but in this case, we raised the temperature to 200 °C, since the kinetics with ethylene were quite slow at 180 °C. Generally speaking, higher selectivity is of course associated with lower temperature, and this is particularly true in the case of formation of thermodynamically less favorable products. Inspection of Tables 8 and 9, however, reveals that at any given level of conversion, with any given pressure of either propene or ethylene, higher temperatures are found to give *greater* fractions of α-olefin. Accordingly, at 200 °C and at the highest pressure of ethylene used (4 atm), an α-olefin yield as high as 250 mM (250 TO) is obtained, a factor of 2.5 greater than any previously reported value in solution.

Computational Results, Discussion, and Overview. Quantum mechanical calculations (DFT, see Experimental and Computational Details) modeling (in vacuo) the ^{iPr4}PCP (**2**) and ^{tBu4}PCP (**1**) systems offer significant insight into the surprisingly high yields of α-olefin obtained in this work, both in solution and solid−gas phase experiments, and enable us to

DOI: 10.1021/jacs.5b05313
J. Am. Chem. Soc. 2015, 137, 9894−9911

Table 8. Dehydrogenation of *n*-Octane [6.2 M][a] Catalyzed by 2 (1 mM) under Varying Propene or Ethylene Pressures at 180 °C (Spinning Reaction Vials)[b]

acceptor, pressure	time/min	total olefins/mM[c]	1-octene/mM (Fraction %)	% acceptor conversion (by GC)	dienes/mM
propene	5	340	93 (29%)	18	17
2 atm	10	590	120 (22%)	32	49
"1.2 M"	20	990	120 (14%)	60	150
	30	1240	80 (8%)	82	280
propene	5	270	92 (35%)	10	10
4 atm	10	490	165 (30%)	15	25
"2.4 M"	20	840	146 (20%)	30	90
	50	1455	120 (11%)	60	345
	90	1980	<5	100	750
propene	5	200	70 (37%)	4	10
6 atm	10	500	160 (33%)	9	25
"3.6 M"	30	870	190 (24%)	18	88
	60	1410	190 (16%)	30	250
	120	1860	170 (12%)	46	480
ethylene	10	23	9 (40%)	2	1
2 atm	40	87	35 (40%)	8	2
"1.2 M"	110	210	76 (37%)	17	8
	250	430	130 (32%)	38	25
	480	690	160 (26%)	55	64
	840	1040	160 (18%)	75	150
ethylene	10	12	8 (66%)	-	0
4 atm	40	24	15 (63%)	1	0
"2.4 M"	80	92	62 (67%)	5	1
	200	170	85 (52%)	7	3
	480	430	150 (37%)	17	18
	960	960	210 (24%)	40	100
	1440	1100	200 (21%)	44	140
(**^{tBu4}PCP**)**Ir (1)**	40	< 4	3 (83%)	ND	0
	180	33	20 (67%)	3	0
ethylene	960	156	78 (56%)	15	2
2 atm	2160	455	127 (29%)	35	20
"1.2 M"	5400	1000	130 (15%)	75	135

[a]Concentrations given represent concentrations obtained after the indicated time of heating, followed by cooling of the reaction vessel to 25 °C so that all species are condensed or dissolved into liquid solution phase. [b]Reaction vessels (glass ampules) were oriented horizontally. [c]Most runs were repeated; results given are the average of two or more runs. Reproducibility averaged ±1%.

put the mechanistic hypotheses advanced above on a much firmer footing. Moreover, while we have previously reported that **2** is a more effective catalyst than **1** for several alkane dehydrogenation reactions,[2,6,19] the difference was not as pronounced as in much of the present experimental work; the present set of DFT calculations help explain this observation as well.

In the following, we use hexane/1-hexene as our representative *n*-alkane/1-alkene pair. If we consider the simple case of an *n*-alkane/1-alkene transfer−dehydrogenation cycle, the resting state of either catalyst **1** or **2** is the corresponding 1-alkene complex, while the rate-determining step is *β*-H elimination of the 1-alkyl iridium hydride C−H bond addition product (Schemes 3 and 4). For (^{tBu4}PCP)Ir, **1**, the difference in free energy between the 1-alkene complex resting state and the rate-determining TS (RDTS) is calculated to be 34.1 kcal/mol (38.9 − 4.8 kcal/mol) at 220 °C (ΔG_{220}; most of the experiments in this work were conducted at 200 or 240 °C and for convenience, free energies are given at the intermediate temperature, 220 °C; Scheme 3). For catalyst **2** (Scheme 4), the difference in free energy between the RDTS for dehydrogenation and the 1-alkene complex resting state is ΔG_{220} = 33.1 kcal/mol (25.4 − (−7.7) kcal/mol); the computed difference between the two catalysts, $\Delta\Delta G_{220}$ = 1.0 kcal/mol, is consistent with the experimentally observed significant but not extreme difference in catalytic activity of **2** vs **1** for *n*-alkane/1-alkene transfer−dehydrogenation.[6]

However, catalyst **1** binds much more strongly to ethylene than to *α*-olefin ($\Delta\Delta G_{220}$ = 8.4 kcal/mol, Scheme 3). The overall barrier for dehydrogenation in the ethylene reaction ($G_{\text{TS-beta-elim}} - G$(**1-ethene**)) is therefore very high, ΔG_{220} = 42.5 kcal/mol. In the case of the less crowded catalyst **2**, ethylene binds only 3.9 kcal/mol more strongly than does 1-hexene, and ΔG_{220} for the ethylene complex vs the *β*-H elimination RDTS is 37.0 kcal/mol. Thus, in comparing catalysis by **2** vs **1**, $\Delta\Delta G_{220}$ = 5.5 kcal/mol in the case when ethylene is the acceptor; this corresponds to a very large difference in reaction rate between the two catalysts, in accord with observations (see Table 8, for example).

Both catalysts **1** and **2** are kinetically highly regioselective for the dehydrogenation of *n*-alkanes to give *α*-olefins;[8] however, due to subsequent double-bond isomerization, with neither catalyst (nor with any other alkane dehydrogenation catalyst) have *α*-olefin yields previously been reported above 100 mM.[8] The following computational results may explain why the conditions in the present work afford much higher *α*-olefin yields, in solution and especially in the solid−gas system.

DOI: 10.1021/jacs.5b05313
J. Am. Chem. Soc. 2015, 137, 9894−9911

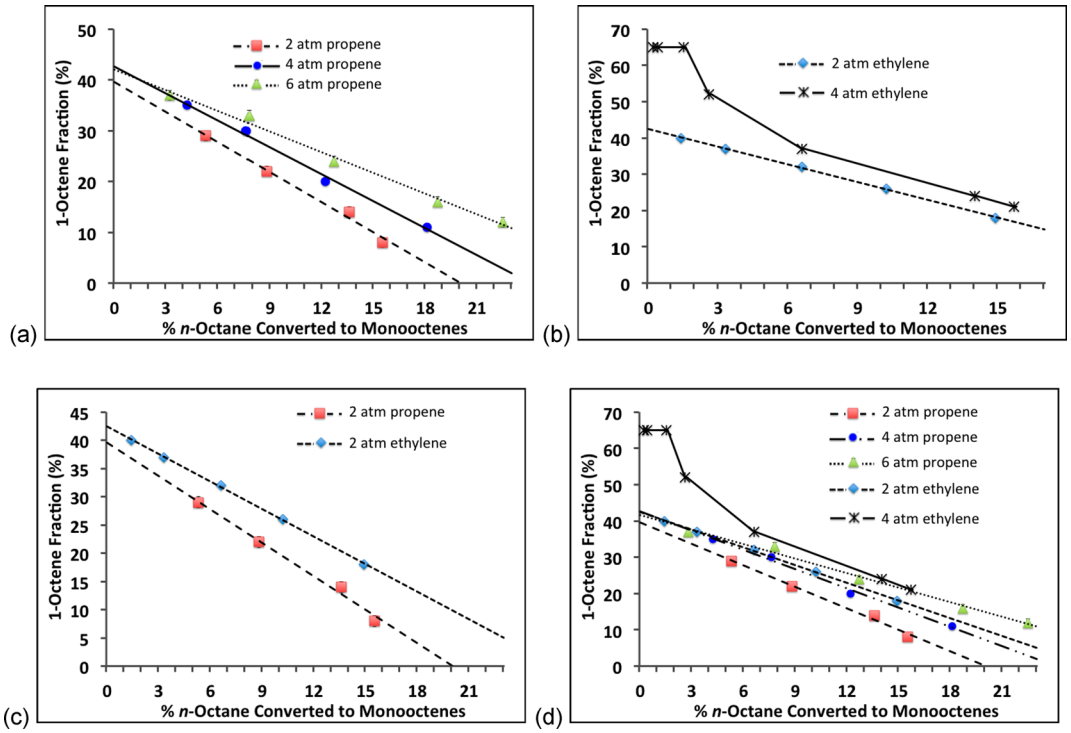

Figure 6. Plot of 1-octene as percentage fraction of octenes formed in the dehydrogenation of *n*-octane catalyzed by **2**-C_2H_4 at 180 °C under (a) 2, 4, and 6 atm propene, (b) 2 and 4 atm ethylene, (c) 2 atm ethylene and propene, (d) data from all plots combined.

Table 9. Dehydrogenation of *n*-Octane (6.2 M)[a] Catalyzed by 2 (1.0 mM) under Propene at 160 °C, and under Ethylene at 200 °C[b]

acceptor	conditions	time/min	total olefins/mM[c]	1-octene/mM (selectivity %)	% acceptor conversion (by GC)	dienes/mM
		10	96	55 (57%)	5	0
	160 °C	20	190	76 (41%)	9	3
propene	2 atm	40	450	100 (24%)	23	21
	"1.2 M"	90	720	105(16%)	40	66
		180	1310	52 (5%)	90	340
		10	55	37 (67%)	1	0
	160 °C	20	118	55 (47%)	2	2
propene	6 atm	40	270	110 (40%)	4	7
	"3.6 M"	80	540	120 (25%)	11	40
		120	690	140 (22%)	12	50
		180	850	140 (19%)	20	110
		10	170	90 (56%)	16%	2
	200 °C	20	360	140 (40%)	23%	14 ± 1
ethylene	2 atm	40	580	200 (40%)	45%	28 ± 1
	"1.227 M"	90	950	195 (24%)	75%	96 ± 2
		120	1190	2(<1%)	100%	206 ± 6
		10	40	28 (74%)	2%	1
	200 °C	40	180	96 (56%)	7%	4 ± 1
ethylene	4 atm	80	390	170 (44%)	17%	13 ± 1
	"2.45 M"	120	560	210 (40%)	25%	30 ± 4
		180	770	250 (34%)	32%	55 ± 1
		280	910	230 (27%)	38%	55 ± 1

[a]Concentrations given represent concentrations obtained after the indicated time of heating, followed by cooling of the reaction vessel to 25 °C so that all species are condensed or dissolved into liquid solution phase. [b]Reaction vessels (glass ampules) were oriented horizontally. [c]Most runs were repeated; results given are the average of two or more runs. Reproducibility averaged ±1%.

As discussed above, we have previously determined that the major pathway for olefin isomerization by **1**[57] proceeds via formation of an iridium allyl complex (involving addition of the allylic sp^3 C−H bond to 14-electron fragment **1**). While allyl-based olefin isomerization pathways have long been known,[58−64] the more commonly proposed "hydride isomerization pathway" involves insertion into a metal-H bond, followed by β-H elimination at the adjacent position (e.g., 2,1-addition of M−H to an α-olefin), and then 2,3-elimination.[63−71] This mechanism would seem to be a particularly likely path for

DOI: 10.1021/jacs.5b05313
J. Am. Chem. Soc. 2015, 137, 9894−9911

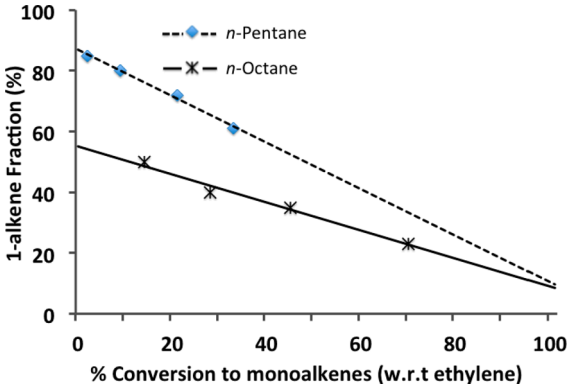

Figure 7. Plot of 1-alkene as percentage fraction of alkenes formed in the dehydrogenation of *n*-octane and *n*-pentane catalyzed by **2-C_2H_4** at 200 °C under 2 atm ethylene.

a transfer-dehydrogenation system in which insertion of olefin (the acceptor) into M−H bonds is a necessary part of the catalytic cycle. The computational results shown in Scheme 3, however, explain why the "allyl isomerization pathway" predominates for isomerization catalyzed by **1**.

Dehydrogenation of *n*-alkane substrate yields (pincer)IrH_2. The predicted importance of the hydride isomerization pathway can be expressed in terms of the three possible reactions of the dihydride (Scheme 3). The RDTS for the hydride isomerization pathway by ($^{t\text{Bu4}}$PCP)IrH_2 (**1-H_2**) (3,2-β-H-elimination) has a free energy of 44.0 kcal/mol (all energies are expressed relative to the free (pincer)Ir complex plus appropriate substrates unless noted otherwise). Alternatively, **1-H_2** can hydrogenate acceptor to complete one catalytic cycle. The respective RDTS free energies for hydrogenation are much lower: 26.0 or 36.4 kcal/mol for ethylene or propene, respectively, and 38.9 kcal/mol for higher α-olefin acceptors (the reverse of the β-H elimination step in dehydrogenation). Thus, the calculations predict that isomerization by **1-H_2** would be negligible in the presence of these acceptors. Even if the barrier to hydrogenation of the acceptor were much higher, as is calculated in the case of TBE at 47.0 kcal/mol, back reaction with the α-olefin product (G_{RDTS} = 38.9 kcal/mol) followed by isomerization via the allyl path (G_{RDTS} = 34.7 kcal/mol) would be much more rapid than isomerization by the hydride path.

In the case of catalyst **2**, the free energy of the RDTS for the hydride isomerization path is much lower (26.2 kcal/mol, Scheme 4) than that of **1** and, importantly, in contrast with **1**, much lower relative to the competitive hydrogenations of acceptor or α-olefin. As with **1-H_2**, hydrogenation of ethylene still has RDTS of much lower energy (18.4 kcal/mol); but for the much less crowded dihydride **2-H_2**, the RDTS for hydrogenation of propene (25.3 kcal/mol) and for the back reaction with α-olefin (25.4 kcal/mol) are quite comparable to the hydride isomerization RDTS. The calculations thus indicate that for catalyst **2** in the presence of ethylene, or in the limit of very high propene concentration or pressure, isomerization via the hydride path will not play a large role. In the case of low propene concentration or pressure, however, or in the case of an acceptor with a higher barrier to hydrogenation (e.g., TBE), the hydride isomerization path can be significant. Moreover, at lower concentrations of propene or in the case of a

Scheme 3. Calculated Pathway with Relative Free Energies (220 °C) for Transfer-Dehydrogenation and α-Olefin Isomerization Catalyzed by 1[a]

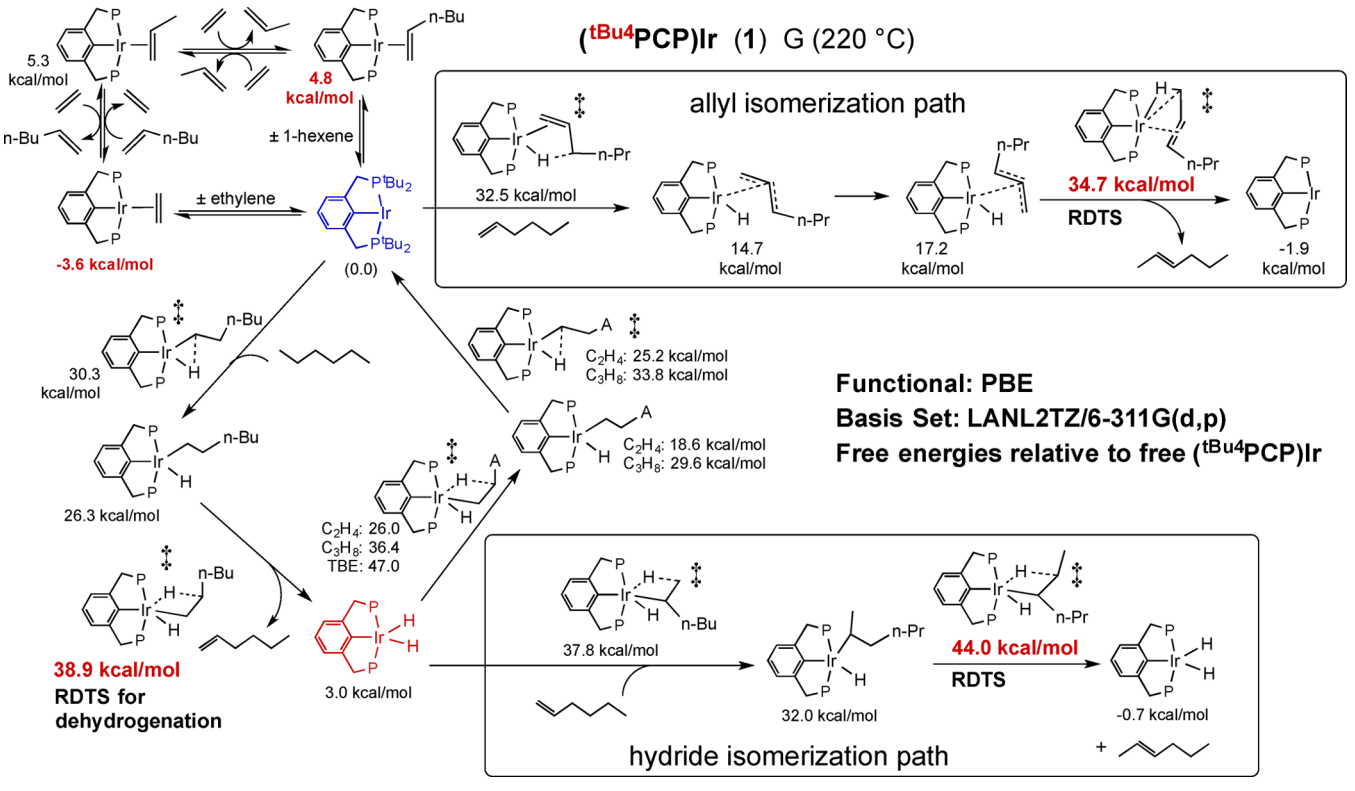

[a]Free energies of key resting states and rate-limiting (determining) transition states (RDTS) shown in red.

DOI: 10.1021/jacs.5b05313
J. Am. Chem. Soc. 2015, 137, 9894−9911

Scheme 4. Calculated Pathway with Relative Free Energies (220 °C) for Transfer-Dehydrogenation and α-Olefin Isomerization Catalyzed by 2[a]

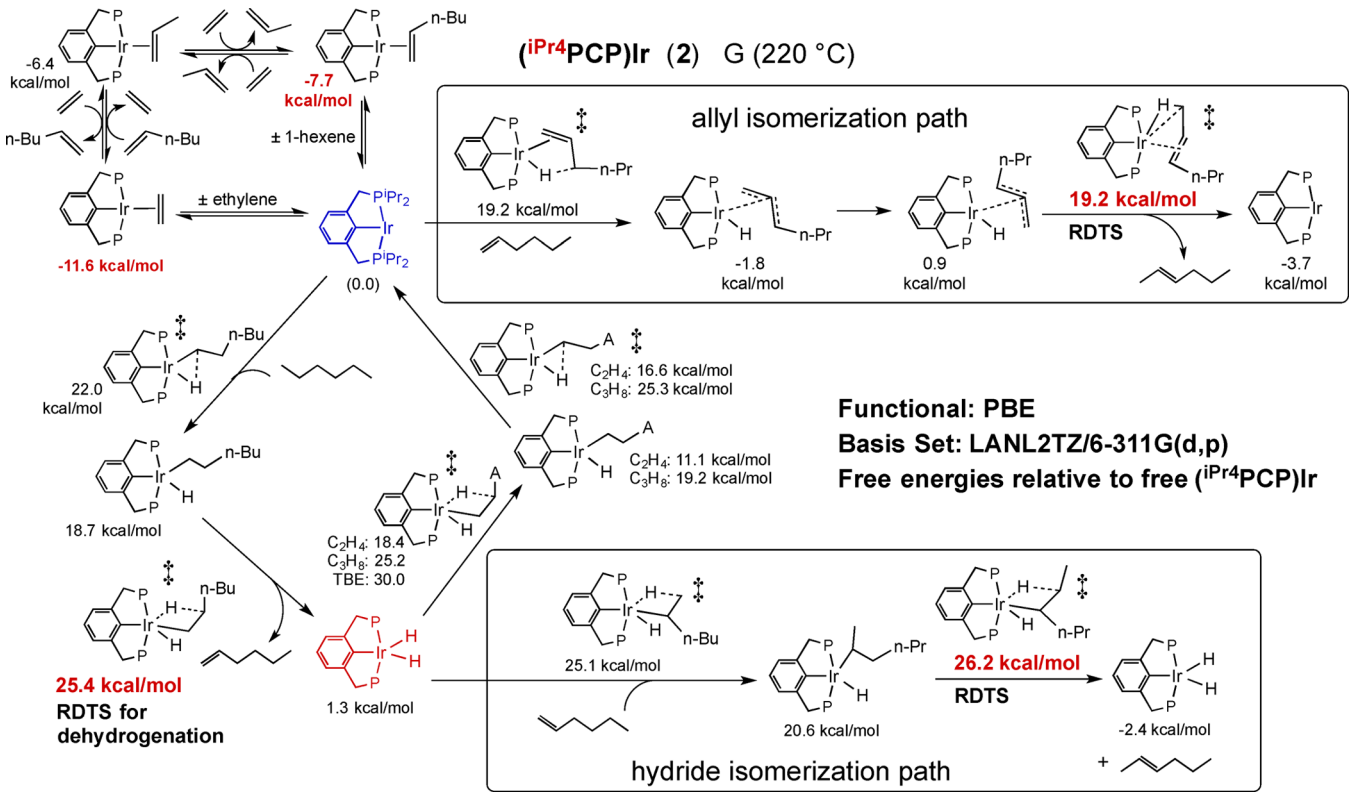

[a]Free energies of key resting states and rate-limiting (determining) transition states (RDTS) shown in red.

Scheme 5. Simplified Scheme Illustrating Relative Rates of Isomerization and Dehydrogenation as Well as Corresponding Rate Constants[a]

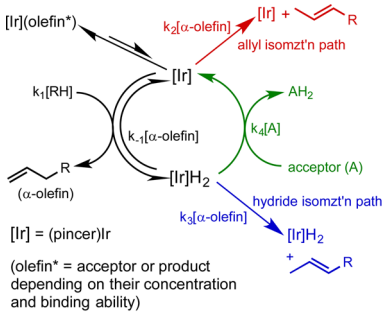

allyl-pathway isomerization: $k_2[\alpha\text{-olefin}][Ir]$

hydride-pathway isomerization: $k_3[\alpha\text{-olefin}][IrH_2]$

net dehydrogenation = $k_1[RH][Ir] - k_{-1}[\alpha\text{-olefin}][IrH_2]$

$$[IrH_2] = \frac{k_1[Ir][RH]}{\{k_{-1}[\alpha\text{-olefin}] + k_4[A]\}}$$

$$\frac{\text{isomerization}}{\text{net dehydrogent'n}} = \frac{k_2[\alpha\text{-olefin}] + \frac{k_3[\alpha\text{-olefin}]k_1[RH]}{\{k_{-1}[\alpha\text{-olefin}] + k_4[A]\}}}{k_1[RH]\left[1 - \frac{k_{-1}[\alpha\text{-olefin}]}{\{k_{-1}[\alpha\text{-olefin}] + k_4[A]\}}\right]} \quad (2)$$

[a]Terms in the numerator of eq 2 are color-coded to indicate their origin in the corresponding isomerization pathways depicted in the scheme.

poor acceptor, the back reaction of α-olefin product will predominate over the forward hydrogenation of acceptor. This back-reaction lowers the net rate of hydrogenation, while isomerization can still proceed via the allyl pathway.

The relative rates of isomerization and dehydrogenation (which determine the ultimate buildup of α-olefin) are expressed algebraically in eq 2, based on the rate constants indicated in Scheme 5.

From eq 2, it can be seen that in the limit of $k_4[A] \gg k_{-1}[\alpha\text{-olefin}]$ and $k_4[A] \gg k_3[\alpha\text{-olefin}]$ (i.e., conditions of fast hydrogenation of the sacrificial acceptor), the isomerization/dehydrogenation ratio reduces to $k_2[\alpha\text{-olefin}]/k_1[RH]$ (eq 3). Equation 3 reflects the competing reactions of (pincer)Ir (present in a very small steady-state concentration) with α-olefin (isomerization) vs alkane (dehydrogenation).

If $k_4[A] \gg k_{-1}[a\text{-olefin}]$ and $k_4[A] \gg k_3[a\text{-olefin}]$:

$$\text{isomerization/dehydrogenation} = \frac{k_2[\alpha\text{-olefin}]}{k_1[RH]} \quad (3)$$

DOI: 10.1021/jacs.5b05313
J. Am. Chem. Soc. 2015, 137, 9894−9911

When ethylene is the acceptor, the difference in free energies of the respective RDTS's is very large for **1**, ca. 13 kcal/mol, and large even for **2** (ca. 7 kcal/mol); thus, either catalyst should be in the fast-acceptor hydrogenation limit and eq 3 is expected to be applicable, with no significant contribution to isomerization from a hydride pathway.

In the case of *propene* acceptor and (^{tBu4}PCP)Ir catalyst (**1**), the difference in free energies for the RDTS of propene hydrogenation vs isomerization via the hydride pathway is also very large (7.6 kcal/mol). The difference between propene hydrogenation vs back-reaction with α-olefin is 2.5 kcal/mol. Hence, as long as propene concentration is comparable to α-olefin concentration the back-reaction rate will be small, and the system will still be in the fast-acceptor hydrogenation limit described by eq 3. Similarly, when α-olefin is used as acceptor, the relative rate of back reaction will be small as long as the acceptor is present in excess.

In the case of propene acceptor and the less bulky (^{iPr4}PCP)Ir catalyst (**2**), however, the calculated difference in free energies for the RDTS of propene hydrogenation vs isomerization via the hydride pathway is small (1.0 kcal/mol), and the difference between propene hydrogenation vs back-reaction with higher α-olefin is negligible (0.2 kcal/mol). In both cases, this represents a competition between the reaction of **2-H$_2$** with propene vs α-olefin. Thus, only in the limit of very high propene concentration or pressure (relative to concentration or pressure of α-olefin) will the isomerization/dehydrogenation ratio approach the lower limit of eq 3. As the reaction progresses and reaches the limit of complete consumption of propene, the isomerization/dehydrogenation ratio will rapidly increase.

Regarding ethylene or propene acceptors, it should be noted that as the overall rate of dehydrogenation is inhibited by their binding to the iridium center, as the acceptor concentration or local pressure is *lowered*, its rate of consumption is *increased*. Thus, *slow* diffusion could result in a (counterintuitive) *faster*-than-expected rate (either in the gas or solution phase) and a self-propagating cycle which in turn could further lower concentrations of acceptor; consecutively, this would result in a higher-than-expected rate of isomerization eq 2 as well as a fast but diffusion-limited rate of hydrogenation.

The use of a higher α-olefin as sacrificial acceptor (one with chain length different from the *n*-alkane substrate so that the reaction is nondegenerate) allows simplification of eq 2, since we can then assume $k_4 = k_{-1}$. If we consider the point at which the acceptor concentration is equal to the product (α-olefin) concentration, eq 2 can be simplified to eq 4:

$$\text{If [}\alpha\text{-olefin acceptor] = [}\alpha\text{-olefin product]:}\quad \frac{\text{isomerization}}{\text{net dehydrogen't'n}} = \frac{2k_2[\alpha\text{-olefin}]}{k_1[RH]} + \frac{k_3}{k_{-1}} \qquad (4)$$

In the case of catalyst **1**, the term k_3/k_{-1} is predicted to be negligible due to the RDTS difference of 5.1 kcal/mol for the respective steps. For **2**, the calculated difference (0.8 kcal/mol) is small, even within the range of error of the calculations, consistent with a significant contribution to isomerization from the hydride-isomerization pathway under this (fairly typical) set of conditions. This is also consistent with the results of the isomerization experiment in which only α-olefin is present (in that case α-olefin of only one chain length is present but that will not affect the rates of isomerization resulting from the different isomerization pathways.)

Note that in the case of catalyst **2** the use of highly reactive acceptors suppresses the dihydride path, which could otherwise play a significant role. But even independent of suppressing the hydride path, in the case of **1** or **2**, higher concentrations of more active acceptors (i.e., high values of k_4[A]) will favor a higher α-olefin fraction of total olefin produced by disfavoring the back-reaction of dihydride with α-olefin product. This is reflected in eq 2 in that, even in the limit of $k_3 = 0$, the ratio of isomerization to net dehydrogenation (eq 2) is still inversely dependent on k_4[A].

(Pincer)Ir-catalyzed alkane dehydrogenation has been of particular interest in the context of alkane metathesis in which (pincer)Ir catalysts operate in tandem with olefin metathesis catalysts.[26] As noted above, the hydride isomerization pathway is suppressed by the presence of effective hydrogen-acceptors in high concentration. In the course of an alkane metathesis reaction, however, the steady-state concentration of olefin is quite low, and the conditions favor the buildup of dihydride complex. Given that both catalyst **1** and **2** dehydrogenate alkanes with high regioselectivity for the terminal position, these results may well explain why catalyst **1** gives much better yields of C_{2n-2} product in alkane metathesis (e.g., *n*-decane from *n*-hexane) than does **2**.[6] Indeed, although **2** and several other catalysts have shown high regioselectivity for dehydrogenation, catalyst **1** has proven nearly unique with respect to good selectivity in alkane metathesis;[6,20,26] a possible explanation is that the dihydride isomerization path in particular is anomalously unfavorable for the highly crowded catalyst **1**.

The effect of the nature and concentration of acceptor on the α-olefin fraction as elucidated above may offer insight into the higher yields of α-olefin obtained in the gas phase vs liquid (Figure 7). In a gas-phase experiment, the ratio of total acceptor to α-olefin present in the reaction vessel equals the relative concentrations of these species to which the catalyst is exposed. In the solution phase experiments, however, while essentially all catalyst and α-olefin are in the solution phase, a large fraction of the ethylene or propene acceptor is in the gas phase, thus biasing the system toward isomerization vs hydrogenation.

We note one additional effect which the DFT calculations suggest would contribute to the high yields of α-olefins reported in this work. High temperature is generally associated with a lack of selectivity. However, the RDTS (β-H elimination) for the dehydrogenation of *n*-alkane by **2** has an enthalpy barrier calculated to be 4.4 kcal/mol greater than that of the RDTS for α-olefin isomerization catalyzed by **2**. Higher temperatures should thus favor dehydrogenation vs isomerization, and ultimately the apparent "selectivity" for α-olefin production. The error in the calculated difference in enthalpy between these very different TSs (allyl-isomerization vs β-H-elimination) is surely large relative to the small difference itself, but taking the calculated value of 4.4 kcal/mol as a "best guess", we can consider the effect of conducting the reaction at 220 °C, for example, compared with a more typical reaction temperature of 150 °C. The predicted change in the ratio of dehydrogenation to isomerization via the allyl pathway is significant, viz. a factor of $\exp[(4.4\ \text{kcal·mol}^{-1}/R)(1/T_1 - 1/T_2)] = 2.1$ ($T_1 = 423$ K; $T_2 = 493$ K). Note, however, that the RDTS for the *hydride* isomerization pathway has a slightly *higher* calculated enthalpy than the RDTSs for the competitive hydrogenation reactions; thus, the hydride pathway will be favored by higher temperature, highlighting further the importance of the use of highly effective hydrogen acceptors in obtaining high yields of α-olefin.

DOI: 10.1021/jacs.5b05313
J. Am. Chem. Soc. 2015, 137, 9894−9911

CONCLUSIONS

We report that pure solid phase (pincer)Ir catalysts are highly effective for the dehydrogenation of *n*-alkanes in the gas phase. (^{iPr4}PCP)Ir (**2**) was found to be particularly effective for this purpose, while commonly used bulkier catalysts such as (^{tBu4}PCP)Ir (**1**) or (^{tBu4}POCOP)Ir are much less effective. High selectivity for α-olefin (the thermodynamically least stable double-bond isomer) is obtained, demonstrating that the solid catalyst is operating as the molecular species. Remarkably, the fractional yields of α-olefin obtained from the heterogeneous systems are actually much greater than have been previously reported with homogeneous solution-phase systems.

In an effort to elucidate the origin of the unusually high α-olefin fraction, as well as the much greater reactivity of the less crowded catalysts, we conducted solution-phase studies and DFT calculations on complexes **1** and **2**. With ethylene as hydrogen acceptor, the much greater reactivity of complex **2** is well explained by the DFT calculations. The difference in energy between the RDTS for dehydrogenation and the ethylene-bound resting state is calculated to be much greater for the bulky complex **1** than for **2**; in the case of higher olefins, the difference is much smaller. This effect is applicable to propene also, but to a much lesser extent. However, decomposition of catalyst **1** seems to be promoted by propene via a mechanism that we do not yet understand.

While both **1** and **2** are known to be regioselective for dehydrogenation of *n*-alkanes to give α-olefins, yields of α-olefin are limited by double-bond isomerization; the highest yield of α-olefin previously reported in solution experiments was 97 mM (obtained with the use of **2**). We have reported that the mechanism of isomerization in the case of catalyst **1** proceeds entirely by reaction of the 14-electron fragment **1** with olefin via an allyl intermediate and not via the more typical hydride class of mechanism. DFT calculations show that the hydride pathway is much more competitive in the case of **2**; this is supported by experiments showing that 1-octene is isomerized ca. 2-fold more rapidly by **2** in *n*-octane vs *p*-xylene solvent (whereas, in the case of complex **1**, the rate of isomerization in these two solvents is identical).

The contribution of the hydride pathway to isomerization is dependent upon a competition for the dihydride complex between hydrogenation of acceptor, hydrogenation of α-olefin (i.e., back-reaction), and 2,1-insertion of the α-olefin leading to isomerization. DFT calculations indicate that the reaction of either **1**-H_2 or **2**-H_2 with ethylene is much more rapid than either back-reaction with α-olefin or isomerization of α-olefin. Hence, the use of ethylene as hydrogen acceptor gives the highest yields of α-olefin in either solution-phase or solid-phase experiments; at high pressures, propene gives α-olefin yields that are comparable. As the calculated activation enthalpy for dehydrogenation is higher than that for isomerization via the allyl pathway, higher temperatures favor the dehydrogenation/isomerization ratio and therefore higher α-olefin yields. Thus, the high α-olefin yields obtained from the gas−solid systems with catalyst **2** are in large part simply a result of the conditions that lead to the gas/solid-phase state: use of highly volatile hydrogen acceptors and the high temperature, both of which mitigate the hydride isomerization pathway. A further advantage of the gas phase is that the catalyst is exposed to the same ratio of acceptor to α-olefin product that is present in the reaction vessel. In contrast, in the solution runs, the volatile acceptors propene and ethylene are partitioned largely into the gas phase while the α-olefin product remains in solution, thus favoring isomerization via the hydride path, as well as hydrogenation of α-olefin (back reaction); both effects contribute to an increase in the ratio of isomerization to dehydrogenation.

Thus, we report a novel molecular gas−solid system which shows high kinetic selectivity for dehydrogenation of *n*-alkanes at the terminal position. The solid phase itself has little if any effect on the intrinsic selectivity and reactivity; indeed DFT calculation modeling the system in vacuo capture the key properties of the catalyst in the gas−solid system as well as in solution. Experiment and calculation have led to greater insight into the factors that determine the yields of the desirable terminal dehydrogenation products. We find that it is possible to effectively eliminate one of two pathways for olefin isomerization with the appropriate conditions and hydrogen acceptor. A focus of further work will be on the design of catalysts for which the remaining η^3-allyl isomerization pathway is less active relative to dehydrogenation.

EXPERIMENTAL AND COMPUTATIONAL DETAILS

General. All manipulations were carried out under an inert atmosphere of dry argon either in a glovebox or using a standard double manifold. (^{tBu4}PCP)IrH_n,[1] (*p*-OMe-^{tBu4}PCP)IrH_n,[72] (^{tBu4}POCOP)IrH_n,[15−18] (^{tBu3Me}PCP)IrH_n,[6] (^{tBu2Me2}PCP)IrH_n,[6] (^{iPr4}PCOP)Ir(C_2H_4),[19] (*p*-OMe-^{iPr4}PCP)Ir(C_2H_4)[6] and (^{iPr4}Anthraphos)Ir(C_2H_4)[73] were synthesized according to literature methods. Anhydrous toluene, anhydrous benzene, anhydrous acetone, anhydrous triethylamine and anhydrous pentane were purchased from Sigma-Aldrich and used as such. Di-isopropylphosphine, [(COD)IrCl]$_2$, and $LiBEt_3H$ were purchased from STREM Chemicals, and dibromo-*m*-xylene was purchased from Fluka. Ethylene used for ^{iPr4}PCPIr(C_2H_4) synthesis was 99.5% pure and was supplied by Matheson. Ultra High Purity Hydrogen from Airgas was used for synthesis of ^{iPr4}PCPIrH_4. For catalytic studies, anhydrous pentane and octane obtained from Sigma-Aldrich was distilled over NaK alloy and stored over 4 Å molecular sieves. Research grade purity (99.999%) ethylene and propylene supplied by Matheson were used for catalytic studies.

Physical Measurements. ^{1}H NMR, ^{13}C(H), and ^{31}P(H) NMR, were recorded on Bruker AMX 400 operating at 400 MHz for ^{1}H NMR, 100 MHz for ^{13}C NMR, and 161.9 MHz for ^{31}P NMR. GC analyses (FID detection) were performed on a Varian 430-GC instrument fitted with Agilent J&W GS-GasPro column (60 m length × 0.32 mm i.d.).

Synthesis of $C_6H_4[CH_2(P^iPr_2)]_2$ (^{iPr4}PCP-H). Dibromo-*m*-xylene (5.00 g, 19 mmol), di-isopropylphosphine (4.5 g, 38 mmol), and triethylamine (10.5 mL, 75.5 mmol) were dissolved in 40.0 mL of THF in the glovebox. The mixture was refluxed under an argon atmosphere for 24 h. The reaction mixture was cooled in an ice bath, and the dense white precipitate was separated by cannula filtration. The solvent from the filtrate was removed under reduced pressure to yield 4.5 g (70%) of colorless oil. ^{31}P(H) NMR (C_6D_6, 161.9 MHz): δ 10.19 (s). ^{1}H NMR (C_6D_6, 400 MHz): δ 6.83−6.92 (m, 4H, Arene *H*), 2.73 (s, 4H, CH_2P)1.32 (d of sept, J_{HH}= 5.6 Hz, J_{PH} = 1.6 Hz, 4H, PC*H*(CH_3)$_2$), 0.73 (d, 5.6 Hz, 12H, PCH(CH_3)$_2$), 0.70 (dd, J_{HH} = 5.6 Hz, J_{PH} = 1.2 Hz, 12H, PCH(CH_3)$_2$).

Synthesis of (^{iPr4}PCP)Ir(HCl/Br). Ultra high purity H_2 was bubbled into a 35.0 mL toluene solution of [(COD)IrCl]$_2$ (3 g, 4.3 mmol) and $C_6H_4[CH_2(P^iPr_2)]_2$ (3 g, 8.8 mmol) for about 15 min. The reaction mixture was then stirred at 80 °C under an H_2 atmosphere for 15 h. Solvent was removed from the resulting red solution to yield a red solid. The red solid was then stirred with 100.0 mL of pentane for 30 min. The solution was cannula filtered and filtrate was collected. The extraction was repeated five more times and filtrate was collected. Then, the residue was further stirred with 100 mL of pentane overnight and extracted. All filtrates were mixed and the

DOI: 10.1021/jacs.5b05313
J. Am. Chem. Soc. 2015, 137, 9894−9911

solvent was evaporated to obtain a red solid in 51% yield (2.6 g). NMR analysis indicated the red solid to be 5:1 mixture of ^{iPr4}PCPIr-(HCl) and ^{iPr4}PCPIr(HBr).

^{31}P NMR (C_6D_6, 161.9 MHz): δ 58.40 (HBr complex, d, 12.3 Hz), δ 58.44 (HCl complex, d, 12.3 Hz).

^{1}H NMR (C_6D_6, 400 MHz): δ 6.95 (s, 3H, Arene *H*), 2.84 (d of vt, J_{PH} = 4.0 Hz, J_{HH} = 17.6 Hz, 2H, C*H*$_2$P), 2.73 (d of vt, J_{PH} = 4.4 Hz, J_{HH} = 17.6 Hz, 2H, C*H*$_2$P), 2.71 (m, 2H, PC*H*(CH$_3$)$_2$), 1.96 (m, 2H, PC*H*(CH$_3$)$_2$) 1.19 (app. Sext (dqt), 7.7 Hz, 12H, PCH(C*H*$_3$)$_2$), 0.86–0.93 (m, 12H, PCH(C*H*$_3$)$_2$), [−36.25 (HCl complex) and −38.25 (HBr complex)] (t, J_{PH}= 13.2 Hz, 1H, Ir*H*).

Synthesis of (^{iPr4}PCP)Ir(C_2H_4). Ethylene was bubbled for about 15 min into a reddish 60.0 mL pentane solution of ^{iPr4}PCPIr(HCl/Br) (0.21 g, 0.4 mmol) whereupon the solution turns colorless. To the above solution was added 1 M LiBEt$_3$H (0.37 mL, 0.4 mmol) dropwise under ethylene atmosphere. The colorless solution then gradually turned brownish. The reaction mixture was stirred overnight under ethylene atmosphere. Removal of pentane from the filtrate obtained from cannula filtration yielded 0.20 g of a brown solid in quantitative yield. NMR and elemental analysis indicated the formation of expected compound in >99% purity. Crystals suitable for X-ray analysis were grown by slow evaporation of a 10 mg solution of (^{iPr4}PCP)Ir(C_2H_4) in 1.0 mL pentane.

^{31}P NMR (C_6D_6, 161.9 MHz): 51.45.

^{1}H NMR (C_6D_6, 400 MHz): 7.45–7.32 (m, 3H, Arene *H*), 3.18 (t, *J* = 3.8 Hz, 4H, C*H*$_2$P), 3.11 (t, *J* = 3.0 Hz, 4H, Ir(C$_2$*H*$_4$)), 2.15 (m, 4H, PC*H*(CH$_3$)$_2$), 1.15 (dd, *J* = 14.7, 7.2 Hz, 12H, PCH(C*H*$_3$)$_2$), 1.00 (dd, *J* = 13.2, 6.7 Hz, 12H, PCH(C*H*$_3$)$_2$).

Calcd for $C_{22}H_{39}IrP_2$: C, 47.38; H, 7.05. Found: C, 48.23; H, 7.23.

Synthesis of (^{iPr4}PCP)IrH$_4$. Introducing H_2 to a pentane solution of (^{iPr4}PCP)Ir(C_2H_4) into atmosphere results in formation of (^{iPr4}PCP)Ir(H_4) in quantitative yields as an orange solid.

^{31}P NMR (*p*-xylene-d_{10}, 161.9 MHz): δ 54.70.

^{1}H NMR (*p*-xylene-d_{10}, 400 MHz): δ 7.02 (s, 3H, Arene *H*), 3.17 (vt, J_{PH} = 4.0 Hz, 4H, C*H*$_2$P), 1.55 (m, 4H, PC*H*(CH$_3$)$_2$), 1.03 (app. qt, 7.5 Hz, 12H, PCH(C*H*$_3$)$_2$) 0.97 (app. qt, 7.1 Hz, 12H, PCH(C*H*$_3$)$_2$), − 9.40 (t, 10.2 Hz, Ir*H*$_4$).

Computational Details. All electronic structure calculations employed the DFT method[74] and the PBE[75] exchange correlation functional. A relativistic, small-core ECP and corresponding basis set were used for the Ir atom (LANL2TZ model);[76,77] all-electron 6-311G(d,p) basis sets were applied to all P, C, and H atoms.[78] The (^{R4}PCP)Ir species was modeled with R = *t*-Bu and *i*-Pr, the phosphine substituents actually used in the experiments. Reactant, transition state and product geometries were fully optimized, and the stationary points were characterized further by normal-mode analysis. Expanded integration grid sizes (pruned (99,590) atomic grids invoked using the integral = ultrafine keyword) were applied to increase numerical accuracy and stability in both geometry optimizations and normal-mode analysis.[79] The (unscaled) vibrational frequencies formed the basis for the calculation of vibrational zero-point energy (ZPE) corrections; standard thermodynamic corrections (based on the harmonic oscillator/rigid rotor approximations and ideal gas behavior) were made to convert from purely electronic (reaction or activation) energies (*E*) to (standard) enthalpies (*H*) and Gibbs free energies (*G*; *P* = 1 atm).[80] *H*, entropy (*S*), and *G* were evaluated at two temperatures, *T* = 25 °C (= 298 K) and *T* = 220 °C (= 493 K). The latter *T* corresponds approximately to the temperature used in the experiments, and all energy values quoted in the principal text refer to *T* = 220 °C unless noted otherwise. In Supporting Information, we tabulate *E*, *H*, *S*, and *G* at *T* = 298 K (*P* = 1 atm) as well as *G* at *T* = 220 °C (*P* = 1 atm). All calculations were executed using the GAUSSIAN 09 series of computer programs.[81]

■ ASSOCIATED CONTENT

Supporting Information

Experimental details including gas chromatographic analysis methods, GC profiles, images of the reaction vessel during the gas-phase reaction, NMR spectra of (^{iPr4}PCP)Ir complexes, X-ray analysis data including cif files, calculated molecular energies and geometries relevant to Schemes 3 and 4. This material is available free of charge on the ACS Publications website at DOI: 10.1021/jacs.5b05313.

■ AUTHOR INFORMATION

Corresponding Authors

*kroghjes@rutgers.edu

*alan.goldman@rutgers.edu

Notes

The authors declare no competing financial interest.

■ ACKNOWLEDGMENTS

This work was supported by NSF through the CCI Center for Enabling New Technologies through Catalysis (CENTC), Grant CHE-1205189, and by Chevron Energy Technology Company. We gratefully thank Jason Hackenberg, Gao Zhuo, and Andrew Steffens for donations of catalyst.

■ REFERENCES

(1) Gupta, M.; Hagen, C.; Flesher, R. J.; Kaska, W. C.; Jensen, C. M. *Chem. Commun.* **1996**, 2083–2084.

(2) Liu, F.; Goldman, A. S. *Chem. Commun.* **1999**, 655–656.

(3) Liu, F.; Pak, E. B.; Singh, B.; Jensen, C. M.; Goldman, A. S. *J. Am. Chem. Soc.* **1999**, *121*, 4086–4087.

(4) Xu, W.; Rosini, G. P.; Gupta, M.; Jensen, C. M.; Kaska, W. C.; Krogh-Jespersen, K.; Goldman, A. S. *Chem. Commun.* **1997**, 2273–2274.

(5) Zhu, K.; Achord, P. D.; Zhang, X.; Krogh-Jespersen, K.; Goldman, A. S. *J. Am. Chem. Soc.* **2004**, *126*, 13044–13053.

(6) Kundu, S.; Choliy, Y.; Zhuo, G.; Ahuja, R.; Emge, T. J.; Warmuth, R.; Brookhart, M.; Krogh-Jespersen, K.; Goldman, A. S. *Organometallics* **2009**, *28*, 5432–5444.

(7) Punji, B.; Emge, T. J.; Goldman, A. S. *Organometallics* **2010**, *29*, 2702–2709.

(8) Choi, J.; MacArthur, A. H. R.; Brookhart, M.; Goldman, A. S. *Chem. Rev.* **2011**, *111*, 1761–1779.

(9) Findlater, M.; Choi, J.; Goldman, A. S.; Brookhart, M. In *Alkane C-H Activation by Single-Site Metal Catalysis*; Pérez, P. J., Ed.; Springer: New York, 2012; Vol. *38*.

(10) Haenel, M. W.; Oevers, S.; Angermund, K.; Kaska, W. C.; Fan, H.-J.; Hall, M. B. *Angew. Chem., Int. Ed.* **2001**, *40*, 3596–3600.

(11) Bezier, D.; Brookhart, M. *ACS Catal.* **2014**, *4*, 3411–3420.

(12) Adams, J. J.; Arulsamy, N.; Roddick, D. M. *Organometallics* **2012**, *31*, 1439–1447.

(13) Adams, J. J.; Lau, A.; Arulsamy, N.; Roddick, D. M. *Organometallics* **2011**, *30*, 689–696.

(14) Shi, Y.; Suguri, T.; Dohi, C.; Yamada, H.; Kojima, S.; Yamamoto, Y. *Chem. - Eur. J.* **2013**, *19*, 10672–10689.

(15) Göttker-Schnetmann, I.; Brookhart, M. *J. Am. Chem. Soc.* **2004**, *126*, 9330–9338.

(16) Göttker-Schnetmann, I.; White, P.; Brookhart, M. *J. Am. Chem. Soc.* **2004**, *126*, 1804–1811.

(17) Göttker-Schnetmann, I.; White, P. S.; Brookhart, M. *Organometallics* **2004**, *23*, 1766–1776.

(18) Morales-Morales, D.; Redon, R.; Yung, C.; Jensen, C. M. *Inorg. Chim. Acta* **2004**, *357*, 2953–2956.

(19) Ahuja, R.; Punji, B.; Findlater, M.; Supplee, C.; Schinski, W.; Brookhart, M.; Goldman, A. S. *Nat. Chem.* **2011**, *3*, 167–171.

(20) Nawara-Hultzsch, A. J.; Hackenberg, J. D.; Punji, B.; Supplee, C.; Emge, T. J.; Bailey, B. C.; Schrock, R. R.; Brookhart, M.; Goldman, A. S. *ACS Catal.* **2013**, *3*, 2505–2514.

(21) Brayton, D. F.; Beaumont, P. R.; Fukushima, E. Y.; Sartain, H. T.; Morales-Morales, D.; Jensen, C. M. *Organometallics* **2014**, *33*, 5198–5202.

(22) Yao, W.; Zhang, Y.; Jia, X.; Huang, Z. *Angew. Chem., Int. Ed.* **2014**, *53*, 1390–1394.

DOI: 10.1021/jacs.5b05313
J. Am. Chem. Soc. 2015, 137, 9894–9911

(23) Jia, X.; Zhang, L.; Qin, C.; Leng, X.; Huang, Z. *Chem. Commun. (Cambridge, U. K.)* **2014**, *50*, 11056−11059.
(24) Goldman, A. S.; Roy, A. H.; Huang, Z.; Ahuja, R.; Schinski, W.; Brookhart, M. *Science* **2006**, *312*, 257−261.
(25) Ahuja, R.; Kundu, S.; Goldman, A. S.; Brookhart, M.; Vicente, B. C.; Scott, S. L. *Chem. Commun.* **2008**, 253−255.
(26) Haibach, M. C.; Kundu, S.; Brookhart, M.; Goldman, A. S. *Acc. Chem. Res.* **2012**, *45*, 947−958.
(27) Dobereiner, G. E.; Yuan, J.; Schrock, R. R.; Goldman, A. S.; Hackenberg, J. D. *J. Am. Chem. Soc.* **2013**, *135*, 12572−5.
(28) Goldman, A.; Ahuja, R.; Schinski, W. U.S. Patent US20130123552A1, 2013.
(29) Steffens, A. M.; Goldman, A. S. Catalytic dehydroaromatization of n-alkanes: Toward a mechanistic understanding and control of product distribution. *Abstracts of Papers*, 245th ACS National Meeting & Exposition, New Orleans, LA, April 7−11, 2013; American Chemical Society: Washington, DC, 2013; INOR-1328.
(30) Goldman, A. S.; Stibrany, R. T.; Schinski, W. L. U.S. Patent US20130090503A1, 2013.
(31) Leitch, D. C.; Labinger, J. A.; Bercaw, J. E. *Organometallics* **2014**, *33*, 3353−3365.
(32) Leitch, D. C.; Lam, Y. C.; Labinger, J. A.; Bercaw, J. E. *J. Am. Chem. Soc.* **2013**, *135*, 10302−10305.
(33) Gupta, M.; Kaska, W. C.; Jensen, C. M. *Chem. Commun.* **1997**, 461−462.
(34) Zhang, X.; Fried, A.; Knapp, S.; Goldman, A. S. *Chem. Commun.* **2003**, 2060−2061.
(35) Chianese, A. R.; Drance, M. J.; Jensen, K. H.; McCollom, S. P.; Yusufova, N.; Shaner, S. E.; Shopov, D. Y.; Tendler, J. A. *Organometallics* **2014**, *33*, 457−464.
(36) Chianese, A. R.; Shaner, S. E.; Tendler, J. A.; Pudalov, D. M.; Shopov, D. Y.; Kim, D.; Rogers, S. L.; Mo, A. *Organometallics* **2012**, *31*, 7359−7367.
(37) Chianese, A. R.; Mo, A.; Lampland, N. L.; Swartz, R. L.; Bremer, P. T. *Organometallics* **2010**, *29*, 3019−3026.
(38) Knapp, S. M. M.; Shaner, S. E.; Kim, D.; Shopov, D. Y.; Tendler, J. A.; Pudalov, D. M.; Chianese, A. R. *Organometallics* **2014**, *33*, 473−484.
(39) Gruver, B. C.; Adams, J. J.; Warner, S. J.; Arulsamy, N.; Roddick, D. M. *Organometallics* **2011**, *30*, 5133−5140.
(40) Adams, J. J.; Gruver, B. C.; Donohoue, R.; Arulsamy, N.; Roddick, D. M. *Dalton Trans.* **2012**, *41*, 12601−12611.
(41) Roddick, D. M. *Top. Organomet. Chem.* **2013**, *40*, 49−88.
(42) Gruver, B. C.; Adams, J. J.; Arulsamy, N.; Roddick, D. M. *Organometallics* **2013**, *32*, 6468−6475.
(43) Allen, K. E.; Heinekey, D. M.; Goldman, A. S.; Goldberg, K. I. *Organometallics* **2013**, *32*, 1579−1582.
(44) Allen, K. E.; Heinekey, D. M.; Goldman, A. S.; Goldberg, K. I. *Organometallics* **2014**, *33*, 1337−1340.
(45) (a) Crabtree, R. H.; Mihelcic, J. M.; Quirk, J. M. *J. Am. Chem. Soc.* **1979**, *101*, 7738−7740. (b) Crabtree, R. H.; Mellea, M. F.; Mihelcic, J. M.; Quirk, J. M. *J. Am. Chem. Soc.* **1982**, *104*, 107−113. (c) Burk, M. J.; Crabtree, R. H.; McGrath, D. V. J. *J. Chem. Soc., Chem. Commun.* **1985**, 1829−30. (d) Baudry, D.; Ephritikine, M.; Felkin, H. *J. Chem. Soc., Chem. Commun.* **1980**, 1243−1244. (d) Baudry, D.; Ephritikine, M.; Felkin, H.; Holmes-Smith, R. *J. Chem. Soc., Chem. Commun.* **1983**, 788−789. (e) Burk, M. J.; Crabtree, R. H.; Parnell, C. P.; Uriarte, R. J. *Organometallics* **1984**, *3*, 816−817.
(46) (a) Galvita, V.; Siddiqi, G.; Sun, P.; Bell, A. T. *J. Catal.* **2010**, *271*, 209−219. (b) Siddiqi, G.; Sun, P.; Galvita, V.; Bell, A. T. *J. Catal.* **2010**, *274*, 200−206. (c) Sun, P.; Siddiqi, G.; Vining, W. C.; Chi, M.; Bell, A. T. *J. Catal.* **2011**, *282*, 165−174. (d) Lobera, M. P.; Escolastico, S.; Serra, J. M. *ChemCatChem* **2011**, *3*, 1503−1508. (e) Solsona, B.; Concepcion, P.; Hernandez, S.; Demicol, B.; Nieto, J. M. L. *Catal. Today* **2012**, *180*, 51−58. (f) Ausavasukhi, A.; Sooknoi, T. *Catal. Commun.* **2014**, *45*, 63−68. (g) Wu, J.; Peng, Z.; Bell, A. T. *J. Catal.* **2014**, *311*, 161−168. (h) Avila, A. M.; Yu, Z.; Fazli, S.; Sawada, J. A.; Kuznicki, S. M. *Microporous Mesoporous Mater.* **2014**, *190*, 301−308. (j) Sui, K.; Yang, M.; Zhou, T.; Guan, Z.; Sun, R.; Han, D. *Integr. Ferroelectr.* **2014**, *154*, 57−63. (j) Shin, H. H.; McIntosh, S. *ACS Catal.* **2015**, *5*, 95−103.
(47) Kundu, S.; Lyons, T. W.; Brookhart, M. *ACS Catal.* **2013**, *3*, 1768−1773.
(48) Lyons, T. W.; Guironnet, D.; Findlater, M.; Brookhart, M. *J. Am. Chem. Soc.* **2012**, *134*, 15708−15711.
(49) Kumar, A.; Goldman, A. S. Pincer based iridium catalysts for light alkane dehydrogenation. *Abstracts of Papers*, 245th ACS National Meeting & Exposition, New Orleans, LA, April 7−11, 2013; American Chemical Society: Washington, DC, 2013; INOR-1202.
(50) Kumar, A.; Mironov, O.; Saxton, R. J.; Goldman, A. S. Pincer iridium catalyzed gas-solid phase and liquid-phase alkane dehydrogenation using acceptors that inhibit olefin isomerization . *Abstracts of Papers*, 248th ACS National Meeting & Exposition; San Francisco, CA, August 10−14, 2014; American Chemical Society: Washington, DC, 2014; INOR-1041.
(51) Ohe, S. *Computer Aided Data Book of Vapor Pressure*; Data Book Publishing Company: Tokyo, 1976.
(52) Ohe, S. Vapor Pressure Calculation, 2015; http://e-data.jp/vpcal1/e/.
(53) Choi, J.; Choliy, Y.; Zhang, X.; Emge, T. J.; Krogh-Jespersen, K.; Goldman, A. S. *J. Am. Chem. Soc.* **2009**, *131*, 15627−15629.
(54) Kundu, S.; Choi, J.; Wang, D. Y.; Choliy, Y.; Emge, T. J.; Krogh-Jespersen, K.; Goldman, A. S. *J. Am. Chem. Soc.* **2013**, *135*, 5127−5143.
(55) Some lead references to organometallic C−H addition, with particular emphasis on selectivity: (a) Bennett, J. L.; Vaid, T. P.; Wolczanski, P. T. *Inorg. Chim. Acta* **1998**, *270* (1−2), 414−423. (b) Wick, D. D.; Jones, W. D. *Organometallics* **1999**, *18*, 495−505. (c) Asbury, J. B.; Hang, K.; Yeston, J. S.; Cordaro, J. G.; Bergman, R. G.; Lian, T. *J. Am. Chem. Soc.* **2000**, *122*, 12870−12871 and references 4−11 therein. (d) Vetter, A. J.; Flaschenriem, C.; Jones, W. D. *J. Am. Chem. Soc.* **2005**, *127*, 12315−12322. (e) Balcells, D.; Clot, E.; Eisenstein, O. *Chem. Rev.* **2010**, *110*, 749−823.
(56) Liu, F.; Pak, E. B.; Singh, B.; Jensen, C. M.; Goldman, A. S. *J. Am. Chem. Soc.* **1999**, *121*, 4086−4087.
(57) Biswas, S.; Huang, Z.; Choliy, Y.; Wang, D. Y.; Brookhart, M.; Krogh-Jespersen, K.; Goldman, A. S. *J. Am. Chem. Soc.* **2012**, *134*, 13276−13295.
(58) Manuel, T. A. *J. Org. Chem.* **1962**, *27*, 3941−3945.
(59) Alper, H.; LePort, P. C.; Wolfe, S. *J. Am. Chem. Soc.* **1969**, *91*, 7553−7554.
(60) Cowherd, F. G.; Von Rosenberg, J. L. *J. Am. Chem. Soc.* **1969**, *91*, 2157−2158.
(61) Misono, M.; Grabowski, W.; Yoneda, Y. *J. Catal.* **1977**, *49*, 363−8.
(62) Casey, C. P.; Cyr, C. R. *J. Am. Chem. Soc.* **1973**, *95*, 2248−53.
(63) Herrmann, W. A.; Prinz, M. In *Applied Homogeneous Catalysis with Organometallic Compounds*, 2nd ed.; Cornils, B., Herrmann, W. A., Eds.; Wiley-VCH Verlag GmbH: Weinheim, Germany, 2002; Vol. *3*, pp 1119−1130.
(64) Crabtree, R. H. In *The Organometallic Chemistry of the Transition Metals*, 5th ed.; John Wiley & Sons: Hoboken, NJ, 2009; pp 229−231.
(65) Mol, J. C. *J. Mol. Catal. A: Chem.* **2004**, *213*, 39−45.
(66) van Leeuwen, P. W. N. M. In *Homogeneous Catalysis: Understanding the Art*; Kluwer Academic Publishers: Dordrecht, 2004; pp 101−107.
(67) Schmidt, B. *Eur. J. Org. Chem.* **2004**, *2004*, 1865−1880.
(68) Otsuka, S.; Tani, K. Isomerization of olefin and the related reactions. In *Transition Metals for Organic Synthesis*, 2nd ed.; Wiley-VCH: Weinheim, 2004; Vol. *1*, pp 199−209.
(69) Seayad, A.; Ahmed, M.; Klein, H.; Jackstell, R.; Gross, T.; Beller, M. *Science* **2002**, *297*, 1676−1678.
(70) Scarso, A.; Colladon, M.; Sgarbossa, P.; Santo, C.; Michelin, R. A.; Strukul, G. *Organometallics* **2010**, *29*, 1487−1497.
(71) Casey, C. P.; Cyr, C. R. *J. Am. Chem. Soc.* **1973**, *95*, 2240−2248.
(72) Krogh-Jespersen, K.; Czerw, M.; Zhu, K.; Singh, B.; Kanzelberger, M.; Darji, N.; Achord, P. D.; Renkema, K. B.; Goldman, A. S. *J. Am. Chem. Soc.* **2002**, *124*, 10797−10809.

DOI: 10.1021/jacs.5b05313
J. Am. Chem. Soc. 2015, 137, 9894−9911

(73) Romero, P. E.; Whited, M. T.; Grubbs, R. H. *Organometallics* **2008**, *27*, 3422−3429.
(74) Koch, W.; Holthausen, M. C. *A Chemist's Guide to Density Functional Theory*; Wiley: New York, 2001.
(75) Perdew, J. P.; Burke, K.; Ernzerhof, M. *Phys. Rev. Lett.* **1996**, *77*, 3865−3868.
(76) Hay, P. J.; Wadt, W. R. *J. Chem. Phys.* **1985**, *82*, 299−310.
(77) Roy, L. E.; Hay, P. J.; Martin, R. L. *J. Chem. Theory Comput.* **2008**, *4*, 1029−1031.
(78) (a) Ditchfield, R.; Hehre, W. J.; Pople, J. A. *J. Chem. Phys.* **1971**, *54*, 724−728. (b) Hariharan, P. C.; Pople, J. A. *Mol. Phys.* **1974**, *27*, 209−214. (c) Krishnan, R.; Binkley, J. S.; Seeger, R.; Pople, J. A. *J. Chem. Phys.* **1980**, *72*, 650−654. (d) McLean, A. D.; Chandler, G. S. *J. Chem. Phys.* **1980**, *72*, 5639−5648.
(79) Frisch, Æ.; Frisch, M. J.; Clemente, F. R.; Trucks, G. W. *Gaussian 09 User's Reference*; Gaussian, Incorporated: Wallingford, CT, 2009; p 147.
(80) McQuarrie, D. A. *Statistical Thermodynamics*; Harper and Row: New York, 1973.
(81) Frisch, M. J.; Trucks, G. W.; Schlegel, H. B.; Scuseria, G. E.; Robb, M. A.; Cheeseman, J. R.; Scalmani, G.; Barone, V.; Mennucci, B.; Petersson, G. A.; Nakatsuji, H.; Caricato, M.; Li, X.; Hratchian, H. P.; Izmaylov, A. F.; Bloino, J.; Zheng, G.; Sonnenberg, J. L.; Hada, M.; Ehara, M.; Toyota, K.; Fukuda, R.; Hasegawa, J.; Ishida, M.; Nakajima, T.; Honda, Y.; Kitao, O.; Nakai, H.; Vreven, T.; Montgomery, J. J. A.; Peralta, J. E. O. F.; Bearpark, M.; Heyd, J. J.; Brothers, E.; Kudin, K. N.; Staroverov, V. N.; Kobayashi, R.; Normand, J.; Raghavachari, K.; Rendell, A.; Burant, J. C.; Iyengar, S. S.; Tomasi, J.; Cossi, M.; Rega, N.; Millam, N. J.; Klene, M.; Knox, J. E.; Cross, J. B.; Bakken, V.; Adamo, C.; Jaramillo, J.; Gomperts, R.; Stratmann, R. E.; Yazyev, O.; Austin, A. J.; Cammi, R.; Pomelli, C.; Ochterski, J. W.; Martin, R. L.; Morokuma, K.; Zakrzewski, V. G.; Voth, G. A.; Salvador, P.; Dannenberg, J. J.; Dapprich, S.; Daniels, A. D.; Farkas, Ö.; Foresman, J. B.; Ortiz, J. V.; Cioslowski, J.; Fox, D. J. *Gaussian 09*, Revision D.01; Gaussian, Inc.: Wallingford, CT, 2009.

DOI: 10.1021/jacs.5b05313
J. Am. Chem. Soc. 2015, 137, 9894−9911